Institute for Visualization and Interactive Systems

University of Stuttgart
Universitätsstraße 38
D–70569 Stuttgart

Masterarbeit Nr. 46

Real-Time Brain Mapping for Treating Substance Abuse using Neurofeedback

Thomas Kosch

Course of Study: Softwaretechnik

Examiner: Prof. Dr. Albrecht Schmidt

Supervisor: Mariam A. Hassib, M.Sc.
Deborah C. Mash, Ph.D.
Dipl.-Inf. Benjamin Jillich

Commenced: June 1, 2015

Completed: December 1, 2015

CR-Classification: H.1.2, H.5.2, H.5.m, I.3.7

Abstract

Physiological sensors attached to a body become more and more integrated into the daily routine of everyone's life. Since physiological sensors become cheaper and more compact, analyzing the state of the body is possible for everyone. Biofeedback describes a practice, that uses physiological sensors to expose the measurements in a visualized manner to the user. This feedback can be used to train mind and body to reach or avoid certain states. A subcategory of biofeedback is neurofeedback, which concerns with brain activity measurements. Brain activity is made available to a corresponding person, so that the person is able to train its brain towards a desired state. A lot of data is produced, which is hard to interpret manually in real-time. Finding patterns to detect neuropsychiatric diseases like Alzheimer, Parkinson or drug addiction requires an extensive analysis of the collected data. This thesis explains what bio- and neurofeedback is and provides an extensive analysis of related research, including a brief introduction about bioelectromagnetism and drug addiction. Furthermore, the effects of drug addiction on the brain will be explained. A big amount of data is generated by the brain activity measurement process. Suitable visualization modalities for interpretation are therefore required. This thesis also presents visualizations of the measured brain activity in real-time to make the data instantly available to a person interested in interpretation. Rather than just visualizing the electrical activity at certain spots, this thesis also proposes a visualization which makes the original electrical source visible which is responsible for the current measurements. This is useful when a person is interested for the reason of electrical activity at certain measurement spots. Neuropsychiatric diseases, especially drug addiction or Alzheimer, can be recognized and treated better. This thesis also explains the used and developed visualization algorithms. The technical realization is explained in detail which includes the implementation of a brain-computer interface, the utilization of an electrode placement system and the verification of the correctness of the implemented algorithms using neuromore Studio as base platform. On top of that, a neurofeedback session for treating drug addiction is performed to evaluate the usefulness of the developed visualizations. Eight participants took part in the study, which showed that the implemented algorithms can be used to interpret the impact of defined situations on the brain. Significant visual changes in brain activation could be found throughout most participants.

Kurzfassung

Am Körper angebrachte physiologische Sensoren integrieren sich immer mehr in den Alltag der Menschen. Begünstigt wird dieser Prozess durch günstiger und kompakt werdender physiologischer Sensoren, die jedem die Analyse des körperlichen Zustands ermöglichen. Biofeedback beschreibt das Benutzen von physiologischen Sensoren, um die gemessenen Werte mit Hilfe einer Visualisierung dem Benutzer zur Verfügung zu stellen. Dieses Feedback kann benutzt werden um bestimmte körperliche Zustände durch Training zu erreichen oder zu vermeiden. Eine Unterkategorie von Biofeedback ist Neurofeedback, welches sich mit dem Messen der Gehirnaktivität beschäftigt. Diese Gehirnaktivitäten werden einer korrespondierenden Person zur Verfügung gestellt, so dass die Person das Gehirn für einen bestimmten Zustand trainieren kann. Eine grosse Menge an Daten wird produziert, was es unmöglich macht diese in Realzeit zu interpretieren. Eine genaue Analyse der gesammelten Daten ist notwendig um neuropsychatrische Krankheiten wie Alzheimer, Parkinson und Drogenabhängigkeit zu diagnostizieren. Diese Arbeit erklärt was Bio- und Neurofeedback ist und bietet eine Literaturrecherche inklusive einer kurzen Einführung in das Themengebiet Bioelektromagnetismus und Drogenabhängigkeit. Ferner wird erklärt wie sich Drogenabhängigkeit auf das Gehirn auswirkt. Aufgrund der grossen Menge an generierten Daten durch das Messen der Gehirnaktivitäten werden geeignete Visualisierungsmodalitäten für die Interpretation notwendig. Diese Arbeit präsentiert Visualisierungen für die gemessenen Gehirnaktivitäten, welche sofort und in Realzeit einer Person zur Verfügung gestellt werden kann. Anstatt nur die Aktivität an bestimmten Messstellen zu visualisieren, bietet diese Arbeit auch eine Visualisierung um den Ursprung elektrischer gemessener Aktivität zu finden, welche für die Messung verantwortlich ist. Dies ist nützlich, wenn eine Person für den Grund einer elektrischen Aktivierung an bestimmten Stellen interessiert ist. Neuropsychiatrische Krankheiten, speziell Drogenabhängigkeit und Alzheimer, können erkannt und effizienter behandelt werden. Diese Arbeit erklärt die benutzten und entwickelten Algorithmen bezüglich der Umsetzung der Visualisierungen. Die technische Umsetzung wird detailliert aufgeführt, welche die Implementierung einer Gehirn-Computer Schnittstelle, die Definition eines Algorithmus zur Platzierung von Elektroden und einer Verifikation für die Korrektheit der implementierten Algorithmen beinhaltet, bei der neuromore Studio als Basisplattform benutzt wird. Eine Neurofeedback Sitzung zur Behandlung von drogenabhängigen Menschen wird vorgeschlagen um die Nützlichkeit der Visualisierungen zu zeigen. Acht Personen nahmen an der Studie teil, welche zeigt, dass die Algorithmen für die Interpretation von Gehirnaktivitäten benutzt werden können. Signifikante visuelle Unterschiede bezüglich der neuronalen Aktivierung konnten bei den meisten Teilnehmern festgestellt werden.

Contents

List of Figures

List of Tables

1 Introduction

I think; therefore I am.

(René Descartes)

Since the age of enlightenment in the 17th century begun, philosopher tried to understand how mind and body work together. René Descartes, a famous philosopher, mathematician, and scientist who lived in the 17th century, stated that the mind and body are completely distinct, further known as mind-body dualism [DC13]. The mind-body dualism is still controversial and could not be proven or rejected [Kim00].

Nowadays, the brain is still not fully researched and it is still unknown how mind and body relate together. New upcoming technologies can be used to understand the behavior of the brain when the body is relaxed or stressed. Physiological sensors can be attached to a body to measure its activity. These measurements can be used to react to the state of a mind or body and deliver feedback. This enabled training of a desired behavior to alter the state of brain and body. The brain and body can be trained to react in a usual manner to these states.

Training mind and body based on the feedback of the used measurement devices is known as biofeedback. Biofeedback aims to measure body activity and exposes the measured data so that a person can react to it and can alter its behavior. For example, biofeedback can be used to treat migraines or headaches [NM07]. Neurofeedback is a specialization of biofeedback, gathering data about brain activity and deliver it to a person. Neurofeedback can also be used to treat neuropsychiatric disorders like autism, depressions or epilepsy [CLM10, LHJ+12, TTH+09]. Bio- and neurofeedback also allow people to learn what happens inside a body in certain situations and provides people an opportunity to create or improve self-awareness.

Physiological sensors and brain-computer interfaces (BCIs) were available to medical applications only due to high price tags and complex usage, which made it difficult to make these sensors available to everyone's life. Many companies and communities changed this during the last years, making bio sensing devices available to private persons. For example, Fitbit[1], JAWBONE[2] and the Zephir Bioharness[3] are breath and hearth rate measurement devices exposing

[1] www.fitbit.com
[2] www.jawbone.com
[3] www.zephyranywhere.com

physiological data to the mind. The OpenBCI[4], the Interaxon Muse[5] and the SenseLabs Versus[6] are only a few of all available brain sensing devices which are affordable for private persons. Recent research uses commercial BCIs to control robots [FR13], annotate videos [SSFP+12] or to detect engagement [AHMG+15].

Neurofeedback can be used to treat neuropsychiatric diseases. Substance abuse and drug addiction is a disease, which alters the way the brain works. The brain feels rewarded after drug consumption and craves for a repetition of this experience [Lyv00, HM01]. Besides of addiction, drugs also cause paranoia, aggressiveness, depressions, impulsiveness or loss of self-control. Since it is possible to measure brain activity using BCIs, differences regarding brain activity can be found within healthy and unhealthy brains affected by drug addiction.

Measuring activity on a scalp can be easily accomplished using physiological sensors. However, these sensors only deliver a current measurement value estimated at the spot of the sensor and do not represent the original electrical source which generated the measured value. Finding the original source of a measured value using physiological sensors is a common problem in bioelectromagnetism known as the inverse problem.

This thesis provides an explanation and implementation of a solution to the inverse problem. The algorithm focuses on finding the spatial origins of electrical sources. This thesis also aims for a real-time visualization, making the original electrical source easily visible to the user. Finding a solution to the inverse problem relies on a suitable sensor placement and the usage of an appropriate BCI. To accomplish this, a standardized electrode placement algorithm is presented and implemented.

The implementation is evaluated with an user study, where a neurofeedback session in combination with virtual reality is presented. We used an OpenBCI for the evaluation together with an Oculus Rift[7] to provide a virtual reality experience. The neurofeedback session aims to reduce drug-related cravings while increasing the concentration of a person. The technical realization is accomplished using neuromore Studio as base implementation.

Overview

This thesis is structured in the following way:

Chapter 2 – Background covers fundamental basics of this thesis.

Chapter 3 – Related Work provides an extensive analysis of related work in the field.

[4] www.openbci.com
[5] www.choosemuse.com
[6] www.getversus.com
[7] www.oculus.com

Chapter 4 – Solving the Forward and Inverse Problem defines the mathematical problem and solution for the implementation in this thesis.

Chapter 5 – Technical Implementation focuses on the technical realization of this project.

Chapter 6 – Evaluation proofs the correctness of the implementation and discusses the gathered results.

Chapter 7 – Conclusion performs a summary about the project and provides improvements for the future.

2 Background

This chapter provides an overview of the brain structures and functionality. This is followed by an in depth discussion of biofeedback and specifically neurofeedback applications which is an integral part of this thesis. Furthermore, several techniques for brain sensing will be presented. This includes electroencephalography (EEG), which will be the base recording technique used in this thesis. The forward and inverse problem are stated in detail which are common problems in bioelectromagnetism. This requires a brief knowledge about electric dipole fields, whose explanation can be found in this chapter. Lastly, the consequences of drug and substance abuse regarding the brain will be explained. After going through the medical and technological topics of this chapter, the reader is prepared for the following chapters.

2.1 Biofeedback

Biofeedback is a technique which uses sensors attached to a human body to measure physiological data and make it available in order to understand physiological processes [Gar76]. This allows the interpretation and manipulation of physiological activities. Biofeedback can be used to understand and modify the physiological and psychological state of a human being. A simple form of biofeedback is the perception of cold and hot. If it is too cold, the body begins to shiver. If it is to hot, the body begins to sweat. Both reactions are a simple form of biofeedback, where the body tells what kind of clothes a person should wear. A person can therefore modify the way it dresses to avoid hot or cold temperatures. In contrast to this simple example, there are many less obvious cases of detecting body reactions like an increased heart rate or the dilation of pupils due some reasons. Biofeedback can therefore help people to detect changing body attributes, which again allow to do preventative measures [Mil78].

Furthermore, biofeedback can be used to modify the behavior of a body. In a first step, biofeedback can be used to understand signals given by a person. In a second step, these signals can be used to activate mechanisms to modify body signals. Regarding to the example of cold and hot, an air conditioner can be controlled by body signals to increase or decrease the temperature.

Biofeedback is mostly a computer-aided practice, where a computer retrieves the data and makes it available in form of feedback using processing techniques or visualizations. Figure 2.1 shows an example of a biofeedback system.

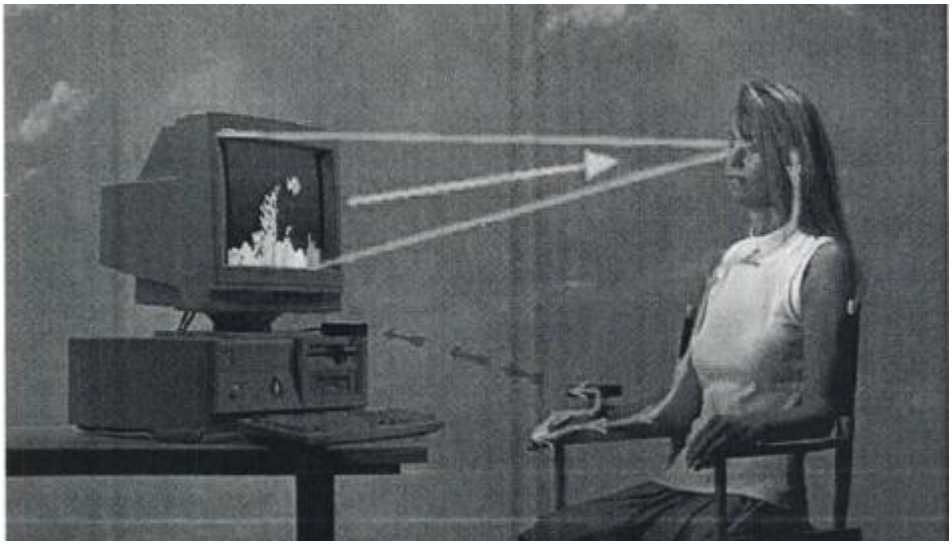

Figure 2.1: A computer-aided biofeedback system [Puc06].

2.2 Neurofeedback

Neurofeedback defines a subcategory of biofeedback using neuronal activities as feedback modality instead of other body modalities. It follows the same principles as biofeedback, which allows measuring brain activities and making the feedback visible to a person [Ham07]. This section will explain how the human brain works and how brain activity can be recognized. Furthermore, different modalities for measuring neuronal activities are going to be presented.

2.2.1 Human Brain Structure

The human brain is one of the most complex organs human possess, giving them the power to think, memorize, imagine and speak. The brain is one of the most researched organs since centuries while researcher are still not able to fully understand it. The structure of a brain can be divided into three parts. The largest part is the cerebrum, which makes up to 90% of the brain mass. The cerebellum is the second largest part and is located below the cerebrum. The cerebellum also connects the spinal cord and the cerebrum. The spinal cord represents the smallest part of the brain and is connected to body functionalities. This includes regulating reflexes, sleeping and blood pressure.

The cerebrum itself is further divided into four lobes. The frontal lobe is located at the front of a brain. It is responsible for reasoning, planning, parts of speech, movement, emotions and problem solving. The occipital lobe is is located at the back of a brain. Its responsibilities lies in processing visual information sent by the eyes. Between the frontal lobe and occipital lobe lies the parietal lobe. It is responsible for movement, orientation, recognition and perception

of stimuli. The last part is the temporal lobe, which lies between the spinal cord and the frontal lobe. Being responsible for perceptions, recognition of auditory stimuli, memory, and speech it allows humans to memorize, comprehend and perceive auditory sensory information [CC91]. The outer surface of the cerebrum is called cerebral cortex. The cerebellum itself is a coordinator of information and provides fine control of movement [Ecc13, MS98]. The spinal cord connects the brain with important body functionalities. Figure 2.2 shows an illustration of all mentioned brain parts.

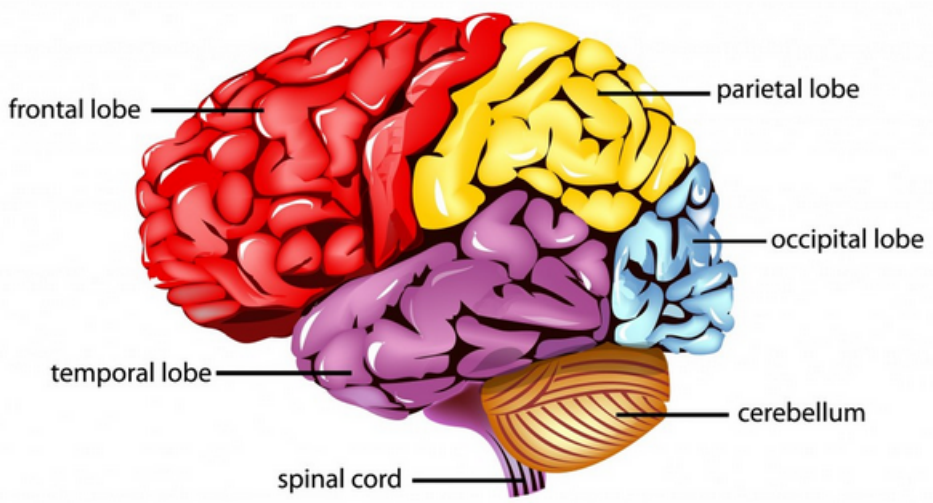

Figure 2.2: Example of a brain model. The upper part shows the cerebrum and its lobes while the lower part represents the cerebellum and its connection to the spinal cord [CS95].

The brain itself is divided into a right and a left hemisphere. Both hemispheres are responsible for different tasks and have a diverged development during the lifetime of a human. The left hemisphere is responsible for analytic thinking, such as making decisions, processing math or speaking. The right side is responsible for creativity and spontaneous actions [DB74]. Humans differ regarding the usage of their hemispheres depending on their age and damaged brain parts. For example, human infants use right hemisphere more intensive until they become older [CJN+97]. It should be noted that a standardized brain for a human does not exist, since the brain structure differs from human to human. This includes brain damages, where people might suffer a lack of social intelligence while improving analytic intelligence at the same time [BCRW+99].

Looking inside the brain, approximately 100 billion nerve cells can be found. These nerve cells are called neurons and are responsible for transporting information to other neurons. All neurons together represent the nervous system. A neuron consists of three basic components which are a cell body containing the nucleus, multiple dendrites and an axon. Figure 2.3 illustrates the structure of a neuron. The nucleus contains genetic material represented in the form of chromosomes. The axon represents a special extension. Instead of receiving signals,

the axon is able to send signals to other neurons with a distance up to one meter. The axon is wrapped with fatty cells called myelin sheath. Like the isolation of an electric wire, the myelin sheath serves as a kind of isolation for the axon. Finally, the axon ending transfers the electrochemical signals to other neurons. Dendrites are an extension of a neuron. They serve as a surface for receiving electrochemical signals from other neurons [Boe].

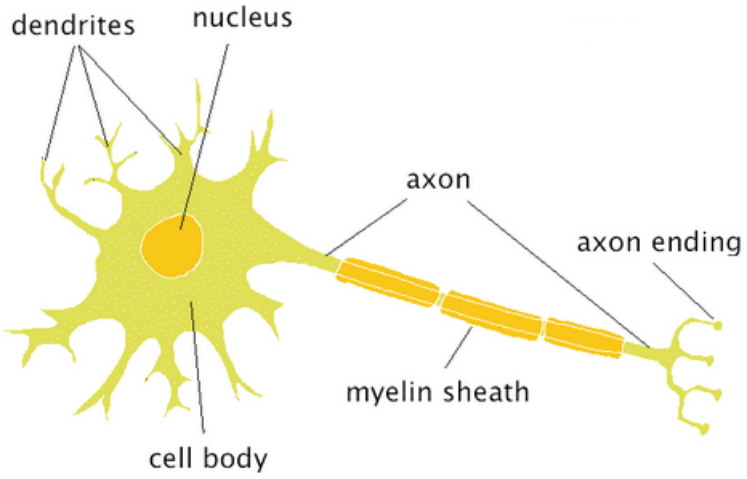

Figure 2.3: Structure of a neuron [Boe].

Between the axon ending and the dendrites of the next neuron is a small gap called synapse. Every neuron has between 1000 and 10.000 synapses. When an electrochemical charge reaches the end of an axon ending, it causes to release tiny vesicles of chemicals. They act as neurotransmitters and are transferred to the next neuron over so called receptor sites. Figure 2.4 shows the concept of a synapse. The exchange of electrochemical charges happens at fast rates, ranging from $0.53\frac{m}{s}$ to $111.76\frac{m}{s}$ [LBZ+00, Boe].

2.3 Brain Activity

Due to electrochemical exchanges between neurons, the generated current can be measured using non-invasive and invasive methods. A non-invasive method refers to an estimation of brain activity using a measurement device on the outer surface of a scalp without operational intervention. Invasive methods describe a operational estimation of brain activity, which requires a placement directly on the brain or deep within it. Invasive brain activity measurements can cause complications and contract diseases [FLRT01]. Recent research states, that invasive measurements can be almost completely replaced using non-invasive measurements by using amplifiers to reduce the impedance of the scalp and therefore increase the signal strength received by neurons [FLRT01].

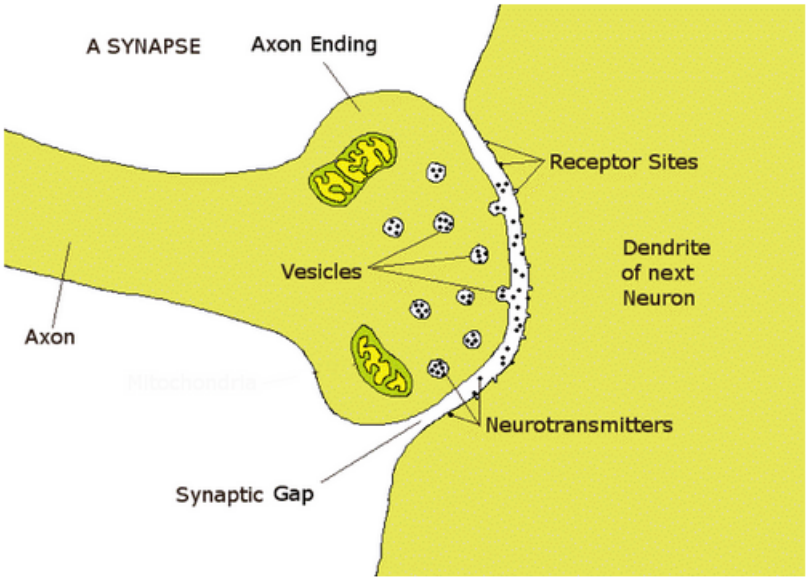

Figure 2.4: Structure of a synapse [Boe].

The focus of this section lies on non-invasive methods, since the measurement and reproduction of results is easier. Furthermore, the principles of electrical and magnetic fields will be explained. Afterwards, two non-invasive methods which enable the measurement of brain activity will be presented. Measurement techniques regarding electrochemical brain activity can be summarized under the term encephalography.

2.3.1 History

The history of brain activity measurements goes back to 1875. An English physician called Richard Caton observed the existence of electrical current of exposed brains from rabbits and monkeys. In 1924, Hans Berger, became interested in a non-invasive way of measuring brain activity. He used his radio equipment to amplify the measured current on a skull and was able to receive weak signals, which were recorded on a strip of paper in the form of a waveform. He observed that the signal pattern is influenced by the state of the subject, for example when the subject has neural diseases [Tep02]. He is the first who used the word electroencephalogram (EEG) for describing brain electric potentials in humans.

Brain signals usually follow a sinusoidal pattern. The measurement unit of the amplitudes is microvolt (μV) while the frequency is measured in Hertz (Hz), which results in a waveform function. The amplitudes normally range from 0.5 μV to 100 μV. The frequency is classified into five different categories, namely alpha, beta, theta, delta and gamma waves. Each category differs in their frequency. Gamma waves have a frequency between 40-100 Hz, Beta waves range between 13-40 Hz, alpha waves between 8-13 Hz, theta waves between 4-8 Hz and

delta waves between 0.5-4 Hz [Tep02]. Figure 2.5 shows the different pattern between alpha, beta, theta and delta waves.

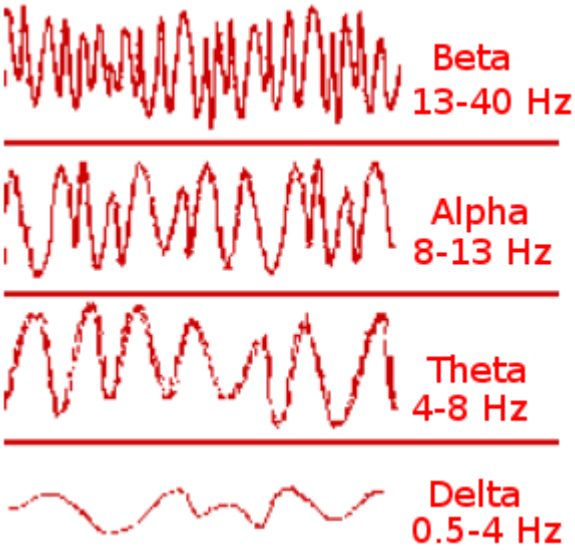

Figure 2.5: Categories of waveform pattern [Tep02].

2.3.2 Electric Dipole Moment

An electric dipole moment describes the measurement of a separated positive and negative charge in a system of electric charges. Both charges have the same magnitude q and are separated by a distance $2a$. Furthermore, $-q$ defines the negative and $+q$ the positive charge of a dipole moment with a vector $\vec{p}$ pointing from $-q$ to $+q$ [SJ13]. The magnitude of the vector $\vec{p}$ is defined as

(2.1) $p \equiv 2a * q$

The measurement unit of the magnitude p is Coulomb-meter (Cm). Figure 2.6 shows the structure of an electric dipole moment.

Electric dipole moments create a electric dipole field. The current flows from the negative charge toward the positive charge. After it reached the positive charge, the current flows back in all directions to the negative charge to build an electric cycle. This creates an electric measurable field [SJ13]. Figure 2.7 shows an illustration of an electric dipole field.

Therefore, electrical signals emitted by neurons create an electrical dipole field. These electrical fields can be measured using invasive and non-invasive methods. In the next section several non-invasive techniques are explained.

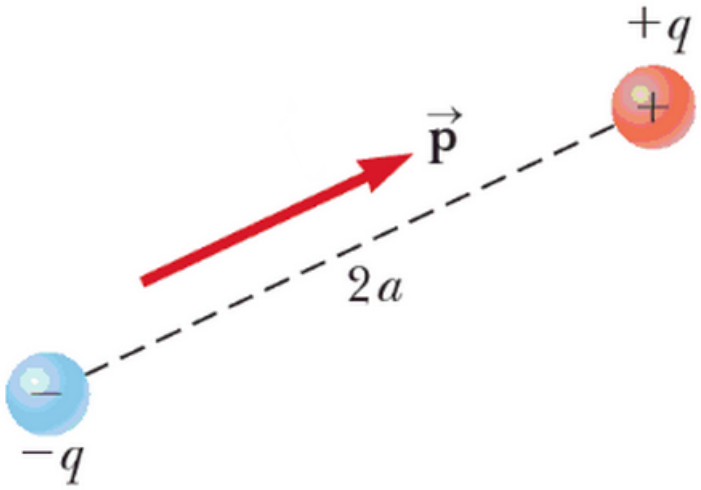

Figure 2.6: A directed dipole moment [SJ13].

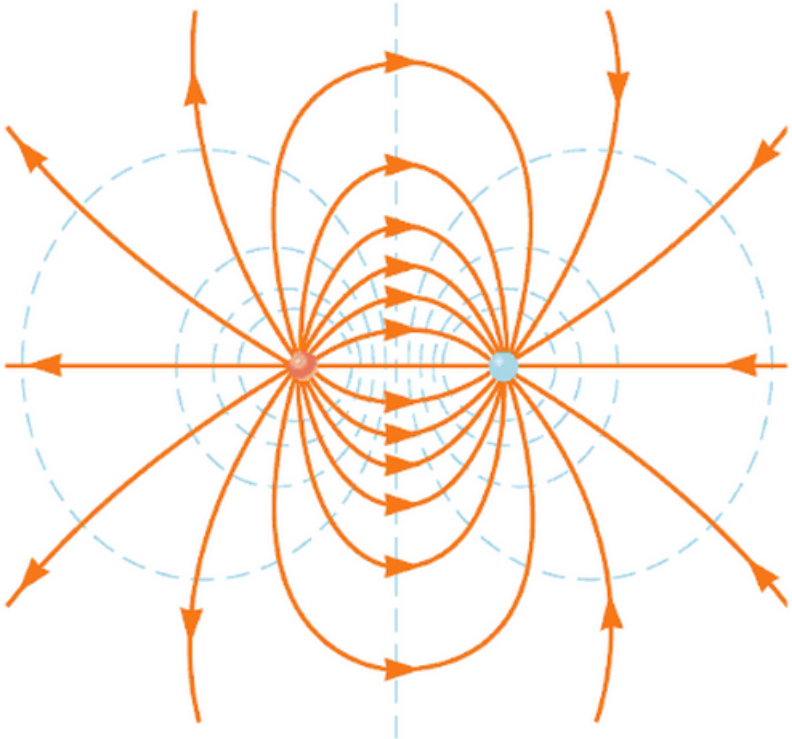

Figure 2.7: An electric field produced by an electric dipole. The blue dotted lines resemble a negative charge while the red dot resembles a positive charge [SJ13].

2.4 Measuring and Recording Techniques

Measuring brain activity triggered by neurons is possible with the help of different sensor modalities. This section covers the Magnetoencephalography and the Electroencephalography, since they are the most used sensor modalities in this field of science [DH01].

2.4.1 Magnetoencephalography

Magnetoencephalography (MEG) is a non-invasive technique for measuring and investigating neuronal activity in human brains. As stated by the Maxwell's equations, electric fields generate magnetic fields which can be measured using MEG [GC99]. In this case, neurons create an electric dipole field which in turn can be expressed as magnetic field. This magnetic field is measurable using a MEG Sensor. Figure 2.8 shows an exemplary MEG measurement device.

Figure 2.8: A typical MEG sensor. The white container-like looking device contains several sensors which allow the measurement of magnetic activity triggered by neurons [HHI+93].

MEG measurements and recording devices suffer several drawbacks. The total number of sensors inside a MEG device is limited. A commercial MEG device contains 37 sensors. Depending on the application more electrodes may be required. Multiple measurements to detect a magnetic pattern somewhere on a scalp are required as well [WLKK91]. Another drawback is the high price of MEG devices.

2.4.2 Electroencephalography

Electroencephalography (EEG) refers to a non-invasive method of measuring brain activity using electrodes, which are able to estimate electric current emitted by neurons in a brain at a specific electrode position [NS05]. The procedure which measures and records brain activity is called electroencephalogram. Figure 2.9 shows an example of a result of an electroencephalogram.

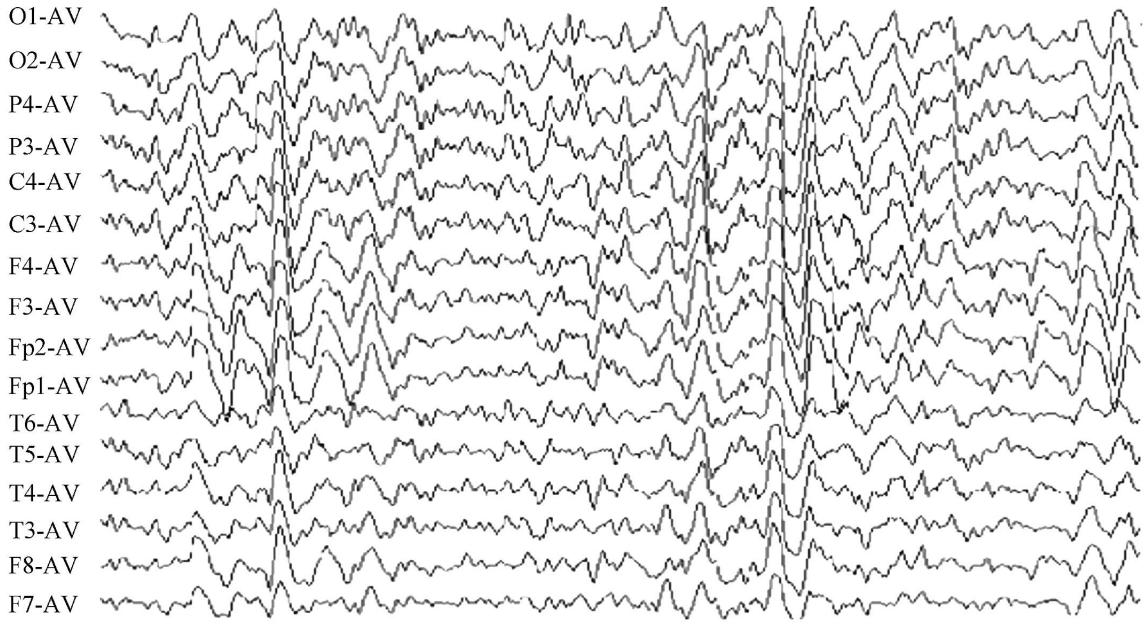

Figure 2.9: An electroencephalogram which records the perceived brain activity on a snip of paper [PZ14].

Obviously, the measured activity does not represent the original position of activated neurons, but the perceived signal strength of neurons at this position. As stated in section 2.4.1, brain activity creates an electromagnetic field. If brain activity is measured using EEG, the activity shows the existence of one or more dipoles in the brain which are the source of the estimated current [NS06].

Investigating a specific part of a brain or using a distribution of electrodes requires a corresponding placement at these spots. Popular distributions are the 10-20 system using 21 electrodes, the 10-10 system using 74 electrodes and the 10-5 system using 329 electrodes [JTD07].

Relative electrode positions on the head are described with an ID. Electrode positions are denoted by an ID and are often described by relative coordinates on a head or by using spherical coordinates [LLPG98]. The 10-20 system denotes a 10% offset based on the head diameter from the nasion, a position on the nose, and from the inion, a position at the back of

the head. Every other electrode position has a offset of 20% based on the head diameter from each other electrode. Figure 2.10 show an example of a relative placement using the 10-20 system. The 10-10 and 10-5 placement system is analog, using 10% offset from the nasion and inion. Afterwards they leave 10% or 5% offset from each other electrode based on the head diameter.

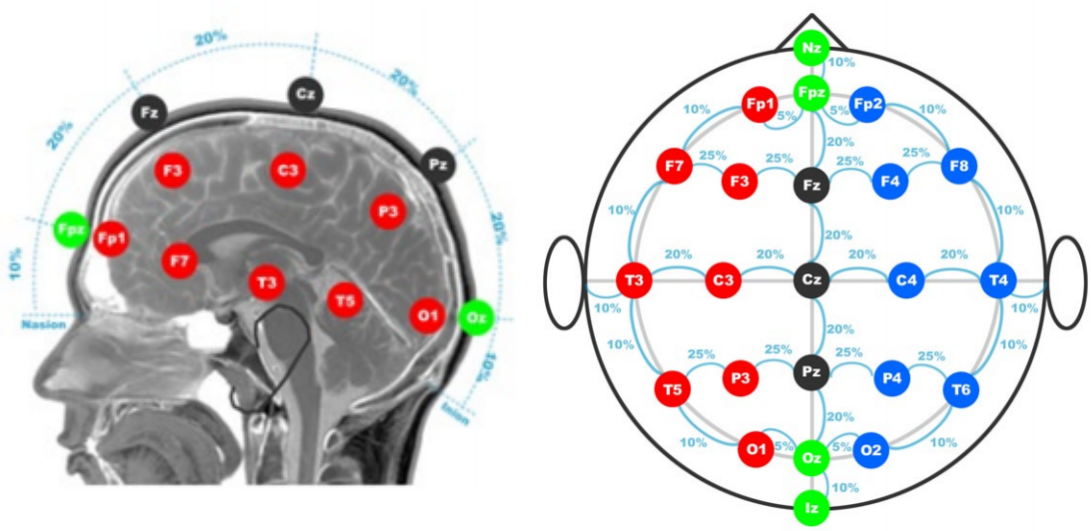

Figure 2.10: Side and top view of a head with the 10-20 electrode placement system. The left image shows a side view of the electrode placement while the right show the top view of it.

2.5 Bioelectromagnetism

Bioelectromagnetism is a field of science which tries to explain electromagnetic phenomena in living beings, like the electromagnetic field generated by a human body using its brain. Lead field theory is a subcategory of Bioelectromagnetism. It tries to explain how the strength of electric activity inside a body is distributed given different paramters, like the strength of the incoming current, the conductivity and the shape of the body part [MP95]. This section explains the lead field theory basics. Furthermore, this section defines the forward and the inverse problem.

2.5.1 Lead Field Theory

Lead field theory is a field of science which concerns with the distribution and sensitivity of electromagnetic signals within a volume conductor. To understand how this works, the term lead vector has to be defined. Consider a point P where a potential field is examined within or

at a volume conductor caused by a dipole $\bar{p}$ at location Q. If we assume that p_x is a unit vector in x direction and that c_x is a coefficient factor in x direction, we can calculate the current potential at a position p_x using the equation

(2.2) $\phi_p = c_x p_x$

The calculation for the y and z direction is equivalent. The overall potential in a point can be calculated with

(2.3) $\phi_p = c_x p_x + c_y p_y + c_z p_z$

A lead vector $\bar{c}$ is a three-dimensional vector, containing relative coefficients, which are depending on the dipole $\bar{p}$ at location Q, the measured potential field at point P, the shape of the volume conductor and the resistance of the volume conductor. Upon these coefficients, the conductivity of the dipole can be estimated. Therefore, the values in the lead vector change for different source estimations in point P. The SI unit of the conductivity is siemens per meter ($\frac{S}{m}$) [MP95].

The lead vector allows to calculate the potential at a position P. The definition of the lead field is an extension to the definition of the lead vector. Instead of defining the conductivity at a defined position, a lead field defines a conductivity with a distribution over a volume conductor. If an arbitrary lead vector on a volume conductor can be calculated, the estimation of a lead field can be estimated using interpolation. The most simple interpolation can be achieved using two electrodes, each mounted at the beginning and end of a volume conductor. The lead vector can then be calculated using the values received from both electrodes, using the resistance and the shape of the volume conductor. Using more electrodes improve the interpolation results [MP95].

2.5.2 The Forward Problem

The forward problem describes the estimation of electric activity at a fixed position on a volume conductor generated by an electrical source. Simplified, the forward problem can be defined as

(2.4) $\phi = KJ$

where ϕ is a vector containing the scalp electrical measurements. K defines the lead field, which depends on the conductivity of the volume conductor and the shape of the volume conductor. J is a vector containing the current dipole moments which generate an electrical source [PM$^+$02]. If a suitable lead field can be defined and the dipole moments are known, the neuronal activity on fixed electrodes can be calculated. Also, the actual current can be measured using electrodes on a volume conductor without any calculations. This can be accepted as possible solution to the forward problem.

In most recent research, a spherical head model is used as volume conductor due to its simplicity. When neuronal activity is measured and noise is neglected, an electric source has to exist somewhere in the brain. But it is still unknown from where the electric source comes from. The inverse problem deals with the estimation of the original electrical source using fix point electrode measurements [HVG+07, MLL99].

2.5.3 The Inverse Problem

In contrast to the forward problem, the inverse problem deals with finding the original electric sources in the brain. This requires the estimation of the actual current on fixed spots on a volume conductor. These measurements can be achieved using electrodes, mounted on fixed points on a volume conductor. As implementing an algorithm to find the solution of the inverse problem is one of the main topics of this thesis, detailed information to solve this will follow in Chapter 4 [HVG+07, MLL99].

2.6 Drug Abuse and Treatment

According to the National Institute on Drug Abuse (NIH) approximately 24.6 million people in the USA are addicted to illicit drugs, alcohol and tobacco[1]. Illicit drugs have a devastating effect regarding the psychological and physiological state of a person. Most drugs are consumed as a stimulant, which encourage productivity, lead to an euphoric state or trigger hallucinations. Most effects caused by drugs are temporary, but leave damage if they are consumed repeatedly, leading to drug addiction. This section discusses the psychological effects of illicit drugs on the brain. Furthermore, the long term effects and established treatment modalities are examined.

2.6.1 Behavior and Brain Affection

Since drugs change the behavior of humans regarding aggressive actions, a decreasing mental state, loss of memory and finally the desire to consume them again, the effects of drugs on the brain is a well researched field of science [HS03, REE08]. It is obvious, that the altering behavior after consuming drugs must have some effect on the human brain, since it changes the way humans think and how they perceive their environment. Doctors acknowledge drugs as a recurring brain disease, which requires recurring treatment to avoid relapses [Les97].

[1] National Institute on Drug Abuse; National Institutes of Health; U.S. Department of Health and Human Services (www.drugabuse.gov/publications/drugfacts/nationwide-trends)

The brain itself has different components, each responsible for different tasks (see section 2.2.1). Most drugs influence the cerebellum, the frontal lobe and the amygdala, a tiny part of the brain located between cerebellum and frontal lobe. Studies have shown, that the frontal lobe is one of the most activated parts of the brain during drug consumption [GV02]. Figure 2.11 shows the typical observed states of a person when consuming drugs.

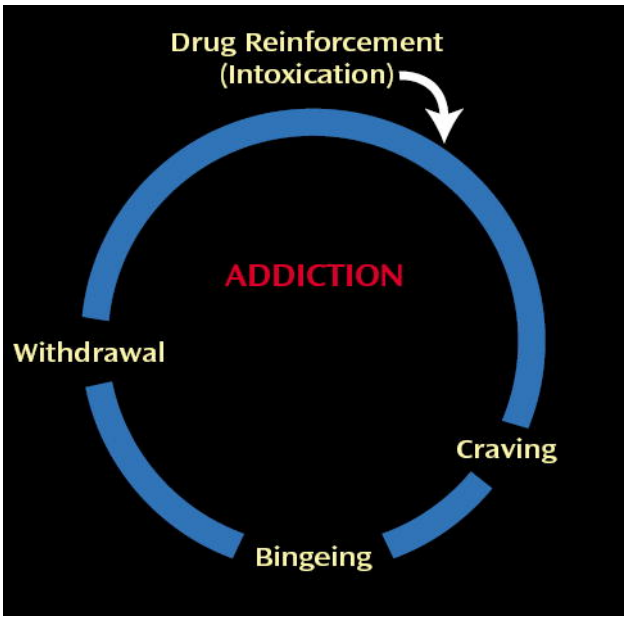

Figure 2.11: The states of a person during drug consumption [GV02].

The frontal lobe and the cerebellum are two motivation related parts of the brain, which use dopamine as neurotransmitter. Dopamine acts as a reward-motivated neurotransmitter. The level of dopamine increases, when drugs like heroin or cocaine are consumed, leading to an euphoric state of the person. Therefore, the motivaion related frontal lobe is affected by consuming drugs. People tend to use drugs again when the level of dopamine sinks to get a rewarded feeling again. Long term usage of drugs lead to depletion of dopamine and therefore increases the risk to damage the brain or getting depressions [RE99].

Drug addiction is accepted as a neuropsychatric disorder which is complex to treat. Even after treatment it is possible to relapse and start consuming drugs again. More important is the insight of a addicted person to accept that the person is addicted. Without this insight, a drug therapy will be most likely useless [ST82].

3 Related Work

With the knowledge from the previous chapter, this chapter will have a look about related research projects regarding neurofeedback, drug treatment in combination with neurofeedback and the estimation of electric dipole moments for brain activity localization. Neurofeedback can be used to get information about mental states, which in turn can be used to react to them. An example are diseases like autism or depression, which can be recognized using neurofeedback. Furthermore, neurofeedback can help to analyze the effects of drug addiction and improve drug related therapies. Finally, similar research projects regarding electric source localization in the human brain will be discussed.

3.1 Disease and Drug Treatment using Neurofeedback

Neurofeedback describes computer-aided information retrieval about the psychological state of an individual person. Since its establishment during the 1960s, it is used to retrain brainwave patterns through operating conditioning. It can be used to train the mental state of a person or as a treatment alternative of learning disabilities, stroke, depression, autism or insomnia [Ham07].

Most project rely on repetitive neurofeedback sessions. A session usually last between 30 and 45 minutes and requires from the participant to accomplish different tasks. Neurofeedback sessions aim to produce desirable brain waves by controlling an activity displayed on a screen. Such an activity can be a computerized game or task. Improvements in brain activity can be rewarded with points to indicate a positive alteration [Oub02]. In most sessions the feedback is exposed in a visualized manner to the participant, for example if a object changes its color. This allows the participant to overcome brain abnormalities by learning to avoid abnormal EEG patterns [SSH07].

Neurofeedback can be used to detect imbalance between neural circuits. This can be achieved using EEG or MEG with real-time imaging capabilities. Imbalanced neural circuits can affect motor functions of the brain which lead to motor diseases like Parkinson. Neurofeedback can be used to alter local brain activity to improve motor functionality. Subramanian et al. developed an approach of treating Parkinson diseased people using neurofeedback [SHJ+11]. They used a colorcoded thermometer to indicate when a person had to squeeze its fingers of their left hand. When the background of the thermometer turned yellow, the participant had

to stop squeezing and rest its fingers for 20 seconds. When the background of the thermometer turned green, the participant had to squeeze its fingers again. As brain activity was recognized, the blue bars filled with red color to visualize brain activity. The results concluded higher motor abilities of the participants when repeating the experiment. Figure 3.1 shows the used thermometer.

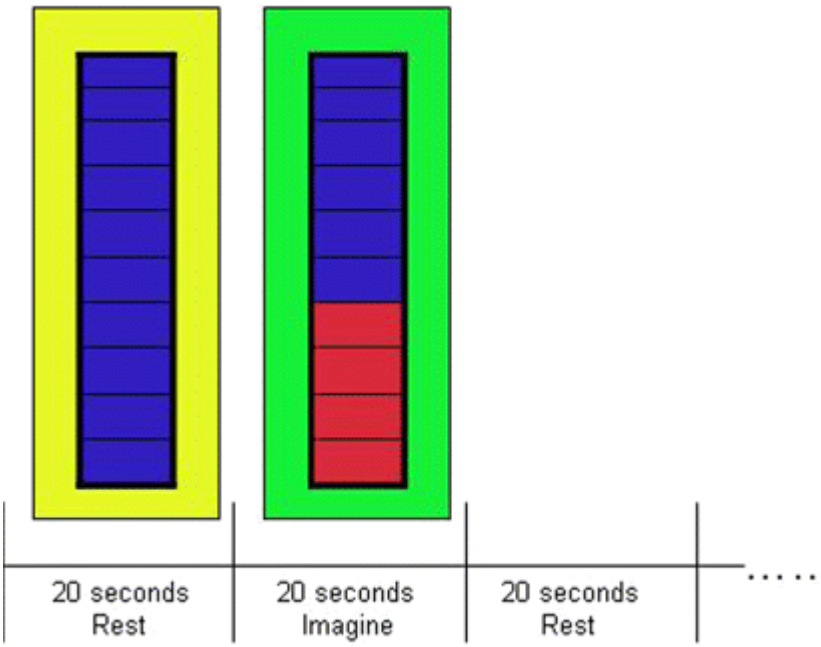

Figure 3.1: The thermometer used for the Parkinson study. A yellow background prompts the participant to rest its hand, while a green background requests the participant to squeeze its fingers. The higher the red bar is, the more brain activity is measured [SHJ+11].

Training the peak alpha frequency for improving cognitive processing speed and executive functions can be achieved as well. Angelakis et al. performed a study which aimed to increase the peak alpha performance of elderly people to a level which is comparable to the peak alpha performance of younger people [ASF+07]. The study was performed with elderly people with an age ranging from 70 to 78 years. Brain activity was measured with EEG using the 10-20 electrode placement system. The participants were asked to do a number of psychometric tests, which were repeated 40 times. The results conclude an improvement in response speed and accuracy during the test. Measured memory capabilities have not improved at all. Figure 3.2 shows the improvement of the alpha peak of three participants.

Obsessive-compulsive disorders (OCD) describe repetitive behaviors by excessive focused thoughts on certain situations. For example, the fear of contamination can trigger an excessive behavior of washing. In other words, it describes actions which last at least one hour a day and interfere with the daily routine of a person [Ste02]. Hammond did first attempts to use

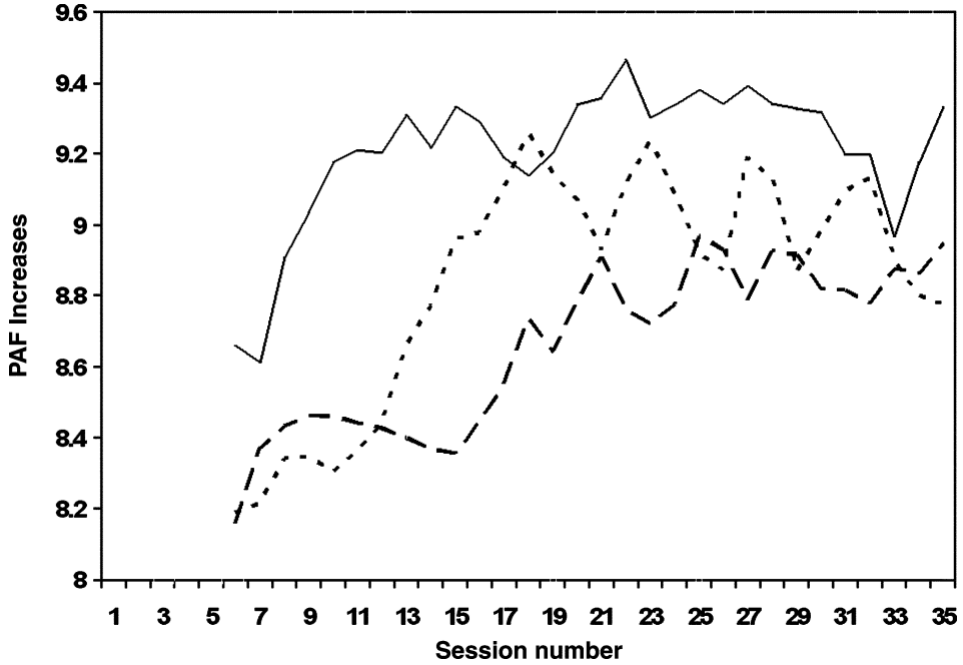

Figure 3.2: The peak alpha performance improves with increasing amount of sessions [ASF+07].

neurofeedback to treat OCD. Using a source localization algorithm, he found out that the left frontal cortex is less active than the right frontal cortex [Ham03]. He could measure an improvement using medical treatment methods regarding improving the left frontal cortex.

Neurofeedback can be used to detect functional brain abnormalities associated with anxiety, depression, panic and post-traumatic stress disorders [HEM95, BSH98]. An activation difference was found between the left and right frontal brain hemisphere. While the frontal cortex of the left hemisphere is activated regarding positive affections and memories, the frontal right hemisphere is more involved by negative emotions [Dav92]. Therefore, the alpha waves in both brain hemispheres are imbalanced, lacking brain activity in the left brain hemisphere. Neurofeedback can be used to train a balanced brain activity distribution in both hemispheres to overcome the effects of depression and anxiety. The neurofeedback sessions must be repeated and help the patient to learn how to balance the brain signals in both brain hemispheres [Ham05].

Determining imbalance between both hemispheres can be estimated using an alpha asymmetric (ALAY) protocol. The received alpha values at the electrodes F3 and F4 are measured. The imbalanced alpha ratio can then be calculated using the formula

$$alpharatio = \frac{F4 - F3}{F3 + F4} \tag{3.1}$$

where a value close to zero indicate a balance between both brain parts [Ham00].

Recent studies have shown, that neurofeedback can be used to treat seizures and propagation of seizures in a brain which cause diseases like epilepsy. Lubar et al. found out that brainwaves between 3 Hz and 8 Hz facilitate the propagation of brain seizures, while brainwaves in the range between 12 Hz and 19 Hz reduce the propagation of the seizure frequency [LSN+81]. Sterman reviewed all of the literature up to 2000 papers and found that almost every neurofeedback study reported positive results regarding epilepsy treatment [Ste00]. Unfortunately, none of these had a permanent effect and therefore it is necessary to repeat the neurofeedback sessions. It is known that many seizure based brain diseases start with normal frequency, jump up to approximately 200 Hz and decline under 1 Hz. This pattern is typical for epilepsy, which can be treated with specialized neurofeedback sessions [WK05].

Gruzelier et al. conducted a study to increase theta waves to alpha waves using a virtual reality environment and a two-dimensional computer screen. Both visualization modalities were compared regarding their learning efficiency. Using a virtual reality environment provided a more immersive and more realisitc experience than a flat computer screen. Also the emitted theta-beta ration improved faster when using virtual reality [GIS+10].

Heinrich et al. could find growing evidence for neurofeedback as a valuable treatment module in neuropsychiatric disorders. They prepared an experiment to treat attention deficit hyperactivity disorder (ADHD) using visual feedback. In a timeframe of eight seconds, a mouse does a pole-vault. The color of the pole is affected by the presence of measured alpha waves and changes its color according to the spectrum blue-white-red. The first two seconds of a pole-vault are used for averaging measured brain waves. The other six seconds affect the color of the pole in correlation to the previous measured mean. Figure 3.3 shows the structure of the experiment. The authors state, that repeated neurofeedback sessions can be used to treat neuropsychiatric disorders [HGS07].

Saxby and Peniston researched the treatment of alcoholism using neurofeedback. The neurofeedback sessions aimed to increase the alpha and theta brainwaves since alpha brainwaves correlate with feeling comfortable while theta brainwaves cause daydreaming and imagery [SP95]. A study with 14 alcoholics was conducted, which had the goal to evaluate the protocol and personal changes. Furthermore, relapses should be avoided. The participants took a 40 minute session once a month. They conducted a total amount of 20 sessions which results in a 20 month long lasting study. One participants relapsed during the study while thirteen stayed sober. The occurrence of alpha and theta brainwaves increased. During the study, depressions were reduced, but the sessions can not guarantee a permanent effect [SP95].

Horrel et al. used neurofeedback to treat addiciton regarding cocaine and marijuana [HEBB+10]. The repeated neurofeedback studies used images that were mapped to categories. Ten participant saw one image after another and should press a button when the shown image could be assigned to this category. A simple example is a neutral category like animals or household. In this case the participant would press the button when an image of a dog or a clock is shown. Additionally, images of drugs were shown. Figure 3.4 shows an example of the set of images used. Goal of the study was to increase the frequency from 13 to 15 Hz

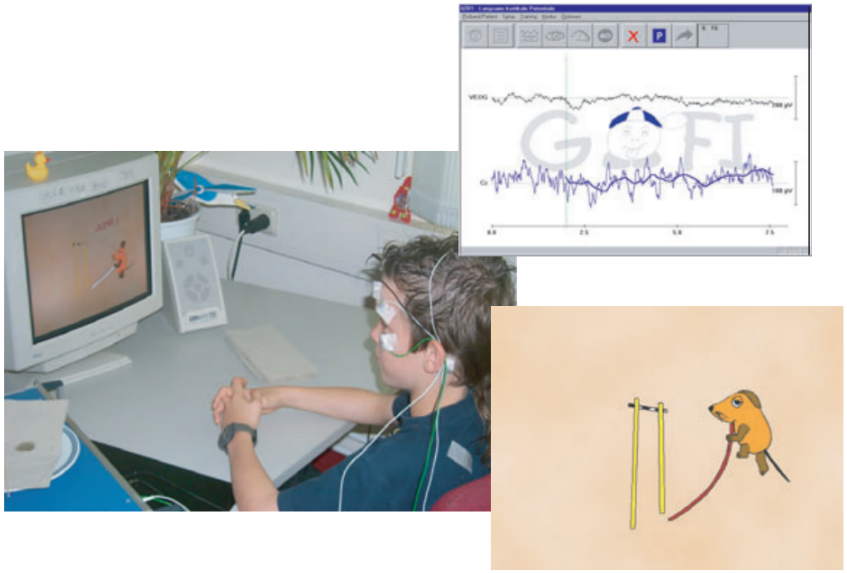

Figure 3.3: Structure of the experiment using a mouse from a popular German TV show. The pole changes its color accordingly to the measured brain waves [HGS07].

and reduce the appearance of theta waves in the left frontal lobe. The participants took part in twelve sessions over six weeks. The results state, that the mean increase of brainwaves was 17.06 % for each participant. Nine from ten participants showed decreased cocaine and marijuana consumption.

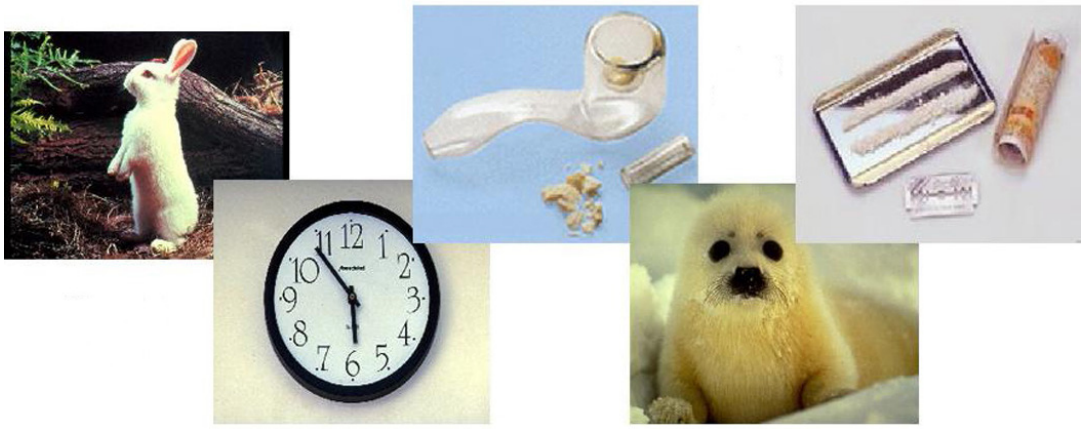

Figure 3.4: Pictograms used in the cocaine study [HEBB+10].

Opiate lead to a calm state, where the brainwaves reside in low frequency. Dehghani-Arani et al. used an audio-visual game, which aims to increase the brainwaves to alpha frequency. While playing the game, the participant could score points while being attentive to the received neurofeedback. Questionnaires were asked before and after playing the game. After 30 sessions

in two months, participants reported decreased anxiety, depressions and physical symptoms regarding drug withdrawal [DARN13].

3.2 Electric Brain Source Localization

Measured electric activity generated by a human body is limited to the spots where MEG or EEG activity is measured. Therefore EEG or MEG represent the current activity at defined spots, but they not reveal the original source of electrical activity. For many cases it would be of interest to know from where electrical sources originate. Many scientists did research regarding the brain localization problem, which deals with finding original electrical sources in a brain. Measuring the electrical current at a specific position is further known as the forward problem, while localizing electrical dipole moments using EEG or MEG measurements is known as the inverse problem. This section comprises related work based on solving the inverse problem and therefore finding original electrical sources in the brain.

Hämäläinen and Ilmoniemi were the first to report an instantaneous distribution of source activity regarding the inverse solution called the minimum norm solution [HI84]. The minimum norm solution uses a two-dimensional space as a base for its calculations and therefore lacks of a three-dimensional space. This leads to a misplacement of estimated electric dipole moments on the deep outer cortex [PM99].

Tarkka et al. used MEG in combination with the brain electrical source analysis (BESA[1]) program to localize dipol moments [TSBP95]. They measured the brain activity of nine participants which were listening to binaural sounds with 85 dB covered with white noise at 60 dB. The recording had 50 high pitches tones which should be counted by the participants. 30 distributed electrodes were used to record the brain activity using MEG. Afterwards the BESA tool was used to analyze dipole moments. This method relies on manual analysis using the BESA tool and therefore can not be used in real time.

Pascual-Marqui et al. developed a Low Resolution Electromagnetic Tomography (LORETA) for localizing dipole moments in three-dimensional space [PMML94]. LORETA uses lead field calculations which include a model of a volume conductor to enable three-dimensional calculations. Furthermore, LORETA tries to minimize possible localization errors of dipole moments. Figure 3.5 shows a snapshot of a visualization generated by LORETA.

However, LORETA was criticized for generating to many localization errors [PMA00], being not able to localize correctly when processing capricious data input [MPL+99]. Other criticized that electrophysiological and neuroanatomical constraints used by LORETA are arbitrary, which in turn have no physiological meaning [KBKE99]. Despite of this criticism, LORETA was used

[1] www.besa.de/downloads/tools/dipole-simulator

Figure 3.5: Example of electrical dipole localization in a brain from the top view. The red areas indicate brain activity [PMLK+99].

successfully in many research projects relying on correct dipole source localization and is acknowledged for correct validation [PMEK+02].

Dale et al. developed a MEG based dipole localization algorithm and compared it to the minimum norm solution. Although the method by Dale et al. generated less errors than the minimum norm solution, localization errors were still present even in noise free environments [DLF+00].

In 2002 Pascual-Marqui developed an improved version of LORETA, called standardized LORETA (sLORETA). sLORETA provides a zero-error localization, hence producing no localization errors in noise free environments. A study has shown that sLORETA has the lowest non-zero localization error compared to the minimum norm solution and to the method proposed by Dale et al. [PM+02].

In 2007, Pascual-Marqui improved LORETA regarding the presence of controlled biological noise, calling it exact LORETA (eLORETA). Since noise can never be fully neglected, eLORETA offers the possibility to use a symmetric weighting matrix to nullify the presence of noise [PM07]. This requires an exact estimation of the current noise. Jatoi et al. compared sLORETA with eLORETA to find the differences in the results of both algorithms. The evaluation was carried out using the sLORETA utility developed by the KEY Institute of Brain-Mind Research in Zurich[2]. The result states that eLORETA has less blur and suppresses less significant details

[2]www.uzh.ch/keyinst

compared to sLORETA, but overall only few differences could be discovered [JKMF14]. Figure 3.6 shows the visual differences between eLORETA and sLORETA from a side view on a head. Figure 3.7 shows the visual differences between eLORETA and sLORETA from a top view on a head.

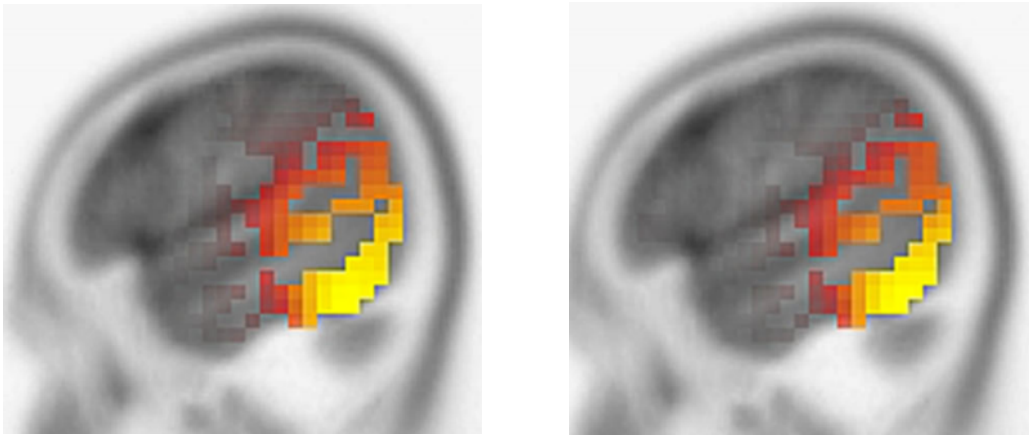

Figure 3.6: Side view of a head using sLORETA and eLORETA. The left image shows a visualization using sLORETA, while the right image shows a visualization using eLORETA [JKMF14].

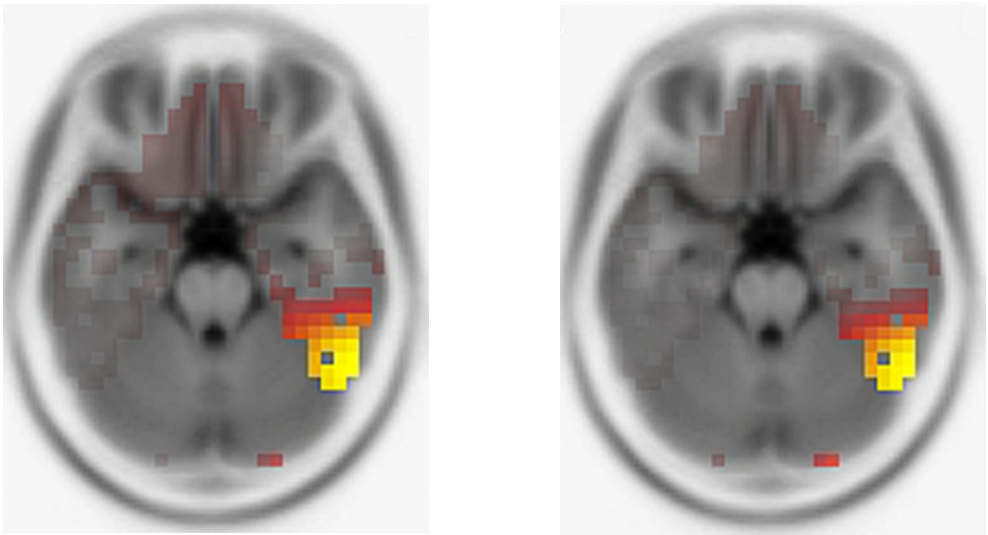

Figure 3.7: Top view of a head using sLORETA and eLORETA. The left image shows a visualization using sLORETA, while the right image shows a visualization using eLORETA [JKMF14].

Other researcher also use LORETA for retrieving and visualizing neurofeedback. Cannon et al. used LORETA for identifying differences of brain activity in the right anterior cingulate cortex to treat drug addiction [CLSB08]. Congedo et al. used LORETA in a experiment which aimed

to increase the alpha and beta brain wave frequency in humans through training [CLJ04]. LORETA is also used to treat and recognize alcohol abuse [Cen14].

4 Solving the Forward and Inverse Problem

The previous chapters discussed how non-invasive brain measurements can be obtained and how these are used in related research projects. This can be done with EEG, which uses electrodes placed on a scalp to retrieve brain activity. This solves the forward problem, which deals with estimating the strength of electric fields on a defined spot generated by an electric source somewhere in the brain. The opposite is the inverse problem. Given some brain measurements, find out where the origin of the electrical source is. Solving this problem reveals the origin of brain activity which helps to understand how the brain reacts to stimuli using neurofeedback. This can help to find brain damages and neuropsychiatric diseases.

This chapter presents algorithms which solve the inverse problem. Furthermore, an algorithm is presented which solves the forward problem in a visualized heatmap manner to show the semantic differences between the forward and inverse problem.

4.1 Solving the Forward Problem

Solving the forward problem can be accomplished by measuring the electric field emitted by the brain using EEG. Electrodes can be placed on a scalp to retrieve measurements. However, depending on the sample rate this produces a lot of quantitative data which is difficult to interpret. A suitable visualization can help to understand and visualize the data in real-time. This section presents an algorithm which is able to process measured brain activity using EEG for calculating pixel-wise magnitudes in a two-dimensional sphere space. A heatmap with an on top view on a head can be used to visualize the results.

4.1.1 A Two-Dimensional Algorithm

Since the forward problem is about estimating the current brain activity at defined electrode places on a scalp, a two-dimensional heatmap algorithm is proposed to visualize the results of the measurements. The algorithm uses sphere coordinates, which are not expressed with a three-dimensional vector, but with two angles called ϕ and θ. If the radius of the sphere and both angles are known, the Cartesian position can be calculated. In this case, the radius of the sphere will be one world unit which is always the maximum. The angle ϕ controls the depth of a defined point on the sphere with $\phi = 0°$ pointing to the top of the sphere and with $\phi = 90°$ to

the bottom of the sphere. θ defines the rotation of a point. Both angles in combination with a radius define a point within a sphere. Figure 4.1 shows an illustrated example of how spherical coordinates can define a point on or in a sphere. This allows calculations in the spherical space. It is assumed that the spherical coordinates of the electrodes and the spherical coordinates of every pixel on the sphere are known.

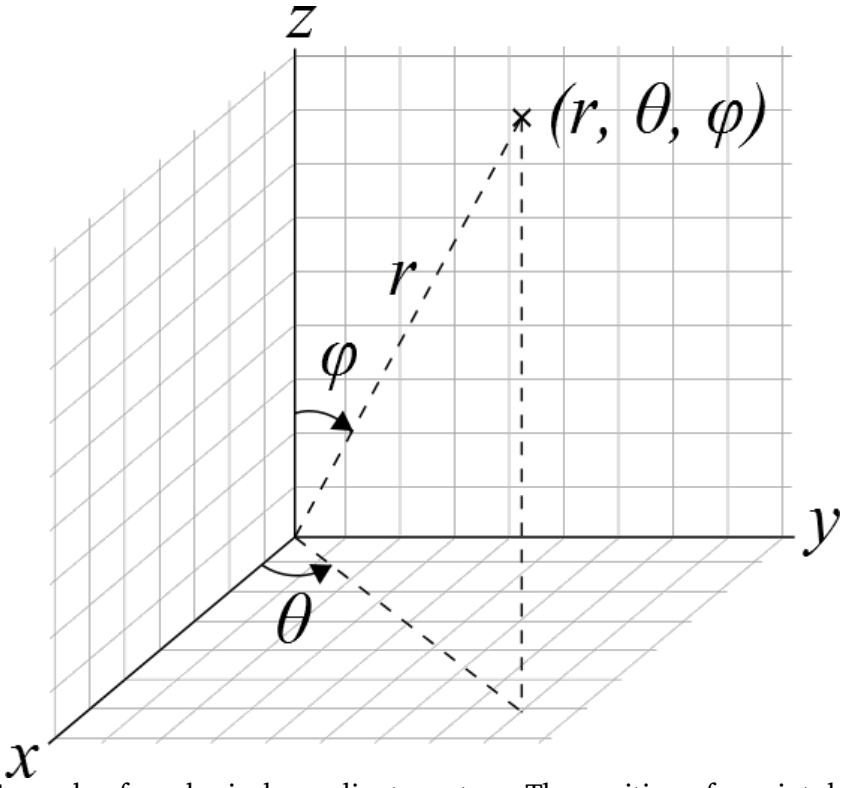

Figure 4.1: Example of a spherical coordinate system. The position of a point depends on the angle ϕ and θ as well as on a radius [Fou].

Using these angles, the corresponding three-dimensional Cartesian coordinate can be calculated. To achieve this, the spherical coordinates must be converted into radians for both the spherical electrode positions and for the current spherical pixel position

(4.1) $\theta_\pi = \theta * \frac{\pi}{180^\circ}$

(4.2) $\phi_\pi = \phi * \frac{\pi}{180^\circ}$

where θ_π and ϕ_π will refer to the corresponding angles converted into radian measure. The letter r expresses the radius. The formulas

(4.3) $x = rsin\phi_\pi cos\theta_\pi$

(4.4) $y = rsin\phi_\pi sin\theta_\pi$

(4.5) $z = rcos\phi_\pi$

calculates concrete Cartesian coordinates in a three-dimensional space. These can be expressed as three-dimensional vector. These Cartesian coordinates can be calculated for every pixel and electrode position. In other words, the algorithm allows us loop over all pixels and electrodes, calculating the distance between each electrode and pixel position to determine the overall impact of all measured electrode signals on one particular pixel. The formula

(4.6) $p = (\sum_{i=0}^{|e|} w_i * e_i) * \frac{1}{\sum_{i=0}^{|e|} w_i}$

with

(4.7) $w_i = \frac{acos(dot(\vec{e_i}, \vec{p}))}{\pi}$

calculates a magnitude for each pixel, where $|e|$ denotes the total amount of electrodes and e_i the currently measured potential at electrode i. The function w_i is a weight function which return value depends on the distance between a pixel. The dot product between the electrode position $\vec{e_i}$ and the current pixel position $\vec{p}$ is calculated to get the cosine angle between them. Afterwards the $acos$ function is used to retrieve the angle in radian measures, whereas the range is defined between $[0; \pi]$. A division through π returns a value between $[0; 1]$. The returned weight can be summed up with every multiplication of each electrode. This in turn is divided by the maximized weight sum. The result is a single scalar for each pixel p which expresses the magnitude in the range between $[0; 1]$.

4.2 Solving the Inverse Problem

While the forward problems can be easily solved using EEG measurements, the inverse problem requires more effort to be solved. The inverse problem deals with finding electric dipole moments in the brain, which are responsible for the current measurement at defined electrode spots. This can be useful for doctors because they do not just see the measured brain activity at certain electrode spots but also the position in the brain which causes the measured electrical activity. This section describes the Low Resolution Electromagnetic Tomography (LORETA) algorithm, which is able to find electrical dipole moments in a brain when the measured electric activities and the head model are known. LORETA is available in three different implementation. This section also discusses all three versions of LORETA.

4.2.1 LORETA (1994)

Pascual-Marqui et al. proposed a first implementation of LORETA in 1994. The algorithm calculates a distribution of active electrical dipole moments in a brain which represent the original electrical source [PMML94]. The calculated distribution should be as smooth as possible and robust to noise regarding the calculated values. LORETA requires the current measured electrical brain activity and a head model as input. The novelty of this approach lies in its three-dimensional nature.

While earlier proposed localization methods work in a two-dimensional space, LORETA is one of the first methods which allow electrical dipole localization within a three-dimensional space. Other proposed methods provided a three-dimensional representation of electrical dipole moments, but the calculations where carried out in a two-dimensional space which lead to localization errors [Ilm93, WGW93]. The LORETA algorithm operates with voxels instead of pixels.

For the formal explanation, the letter E defines the number of electrodes while the letter V defines the number of voxels. In all cases, the superscript T defines the transpose function of a matrix. Formally, for noise-free instantaneous measurements, the forward problem can be defined as

(4.8) $\phi = KJ$

where ϕ is vector of size E containing the current instantaneous scalp measurement. K is a $E \times V$ transfer matrix containing elements $(k_{11}^T, k_{12}^T, \ldots, k_{E,V}^T)$ where k is a lead field defined as a three-dimensional vector. In other words, K is a matrix containing three-dimensional vectors as lead vectors. For example, an infinite homogeneous medium with conductivity σ for a vector k_{ij} can be defined as

(4.9) $k_{ij} = \frac{1}{4\pi\sigma} \frac{r_{Ei} - r_{Vi}}{||r_{Ei} - r_{Vj}||^3}$

where r_{Ei} and r_{Vj} are three-dimensional position vectors for the i-th scalp electrode and the j-th voxel. J is a vector of dimension V, containing the current density of each voxel stored as a three-dimensional vector. More formally, J can be described as $J = (j_1^T, j_2^T, \ldots, j_V^T)^T$. The current density defines the current dipole moments with a vector pointing to the location where its electrical activity emits. K as a transfer matrix, defines the conductivity of each voxel correlated to the conductivity and the head model.

When solving the forward problem using EEG, the vector ϕ as well as the transfer matrix K is known. The vector J has to be solved to get the current density for each voxel. The system of equations is strongly underdetermined because the number of voxels often exceed the number of electrodes with $V \gg E$. Therefore J can have arbitrary solutions. LORETA focuses on finding the smoothest solution by minimizing the following equation with respect to J:

(4.10) $min_J ||BWJ||^2$

W is a diagonal $V \times V$ matrix which is defined as

(4.11) $w_{ii} = ||K_i||$

where K_i is the i-th column of K. The equation

(4.12) $Z = WJ = (z_1^T, z_1^T, \ldots, z_V^T)^T$

returns a vector Z of dimension V containing three-dimensional vectors. Z contains the weighted current density. B is a $V \times V$ matrix containing three-dimensional vectors. It defines the discrete Laplacian operator, defined as

(4.13) $BZ = (I_1^T, I_2^T, \ldots, I_V^T)^T$

I is a vector of dimension V defined for a regular cubic grid of points with

(4.14) $I_i = \frac{1}{d^2} * (6z_i - \sum_p z_p), \forall\ p$ under constraint: $||r_i - r_p|| = d$

with i counting the voxels and p denoting the electrodes. The distance d is calculated between every voxel and electrode. The weights of a voxel are summed up for every electrode and divided by the square of the distance. This value is stored into matrix I. With matrix I defined, equation 4.13 can be solved and matrix B can be retrieved. In a last step, matrix B containing the weighted densities must be multiplied with matrix K to set up a correlation between the head model, conductivity and weighted densities. This solution also has to be inverted. This can be accomplished using

(4.15) $\hat{J} = T\phi$

with

(4.16) $T = (WB^TBW)^{-1}K^T\{K(WB^TBW)^{-1}K^T\}^+$

The superscript $+$ defines the Moore-Penrose pseudoinverse, which can be used to invert singular matrices [Gol12]. The V dimensional vector $\hat{J}$ contains the current density power of each voxel. Each value of the vector $\hat{J}$ is a three-dimensional vector. The magnitude of the i-th voxel can be estimated by calculating the length of the i-th vector of $\hat{J}$.

The first version of LORETA calculates a distribution of electric activity through a brain. The first brain activity experiments using LORETA were recorded as images. Figure 4.2 shows brain activity of a brain using a top view with different slices.

4.2.2 sLORETA (2002)

Natural environments often contain noise which modifiy EEG measurements. LORETA itself does not take noise into account. This may lead to localization errors and blurred results.

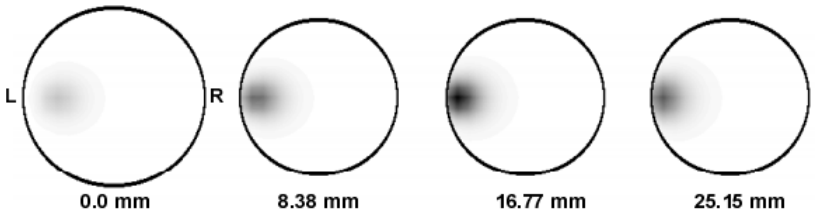

Figure 4.2: Electric dipole localization using LORETA. The circle shows the top view of a head with different slice depths. Black voxel indicate electrical dipole moments. Numbers below the circles define the slice depth [PMML94].

An improved version of LORETA was developed by Pascual-Marqui in 2002 called standardized LORETA (sLORETA) [PM$^+$02]. sLORETA aims to have zero localization errors in the absence of noise and minimal localization errors in the presence of noise. Furthermore, the implementation of sLORETA is easier compared to LORETA.

As in LORETA, the forward problem remains the same

(4.17) $\phi = KJ$

with ϕ containing the current electric scalp potentials, K being the transfer matrix and J being the current density. The following equations returns the current density power for every voxel

(4.18) $\hat{J} = T\phi$

with

(4.19) $T = K^T(KK^T + \alpha H)^+$

where H is a $E \times E$ centering matrix and alpha a constant in the interval $[0; 1]$. The centering matrix is a symmetric and idempotent matrix. If the centering matrix is multiplied with a vector, the result will be the same as if the mean of the vector was subtracted from every component. The centering matrix is defined as

(4.20) $C_n = I_n - \frac{1}{n}11^T$

with I being the identity matrix of size n and 1 being a matrix filled with 1's of size n. The centering matrix averages the result depending of the value of α. A α of zero removes the averaging and the calculation therefore return the result without blurring noise. A greater α increases the intensity of the blurring between every voxel.

Furthermore, noise can be reduced using the variance of the estimate $\hat{J}$ to standardize it. The variance of the estimated density can be calculated using the equation

(4.21) $S_{\hat{J}} = K^T(KK^T + \alpha H)^+ K$

$S_{\hat{J}}$ is a $V \times V$ matrix containing 3×3 matrices due to the vector matrix multiplication with matrix K. The final density power for the voxels with minimizing noise can then be calculated with

(4.22) $\hat{J}_l^T \{(S_{\hat{J}})_{ll}\}^{-1} \hat{J}_l$

where S_{ll} is the estimated variance value denoted as 3×3 matrix at the l-th line and column. J_l denotes the current density power for the l-th voxel. Equation 4.22 returns the magnitude of a voxel as a scalar which describes its current density power.

4.2.3 eLORETA (2007)

sLORETA reduces the appearance of noise in the result set, but it still affects the result in a minimal manner. Pascual-Marqui published 2007 exact LORETA (eLORETA), which extends some equations by a structured block-diagonal weight matrix W [PM07]. Equation 4.19 is extended by matrix W which is a $V \times V$ matrix containing three dimensional vectors

(4.23) $T = W^{-1} K^T (K W^{-1} K^T + \alpha H)^+$

The weight matrix allows further modifications to adjust the result regarding noise. If $W = I$ for I being the identity matrix, the result will not be altered and sLORETA will result. Estimating W can be complicated because it is dependent to the environment.

5 Technical Implementation

The technical realization of this project uses already available libraries and tools with an own developed implementation on top. This chapter briefly mentions and explains facilities which are in use during the implementation of a visualization regarding the estimation of a solution to the forward and inverse problem. This chapter also provides a verification of all presented algorithms to prove the correctness of the implementation.

5.1 Neuromore Studio

Neuromore Studio[1] is a platform which supports the retrieval of signals by brain-computer-interfaces (BCIs), the modification of incoming signals and the creation of neurofeedback sessions. It is able to work with different BCIs simultaneously, generating neurofeedback and providing dynamic feedback using state machines. Received signals can be processed using so-called nodes which retrieve signals from a BCI and process them to a desired output. A set of together operating nodes are called classifier. Figure 5.1 shows a screenshot of the neuromore Studio user interface. Figure 5.2 shows an example of a classifier. As neuromore Studio is providing the base for this project, it is used for the implementation of the visualization algorithms as well as for the evaluation in Chapter 6.

5.2 OpenBCI Integration

The OpenBCI[2] is a bio-sensing microcontroller which is able to sample and measure electrical brain activity. Unlike other BCIs, it delivers the unaltered raw data signal without any modifications like additional smoothing. This allows direct modifications of the raw data. Currently two versions of the OpenBCI exist, with one supporting up to eight electrodes and a second one supporting up to 16 electrodes. The data transfer between a OpenBCI and a PC is accomplished over a Bluetooth connection. The OpenBCI also includes an accelerator which can be used to detect head movements. Head movements cause noise and the corresponding signals can be smoothed when knowing where noise has occurred. During this project, both

[1] www.neuromore.com
[2] www.openbci.com

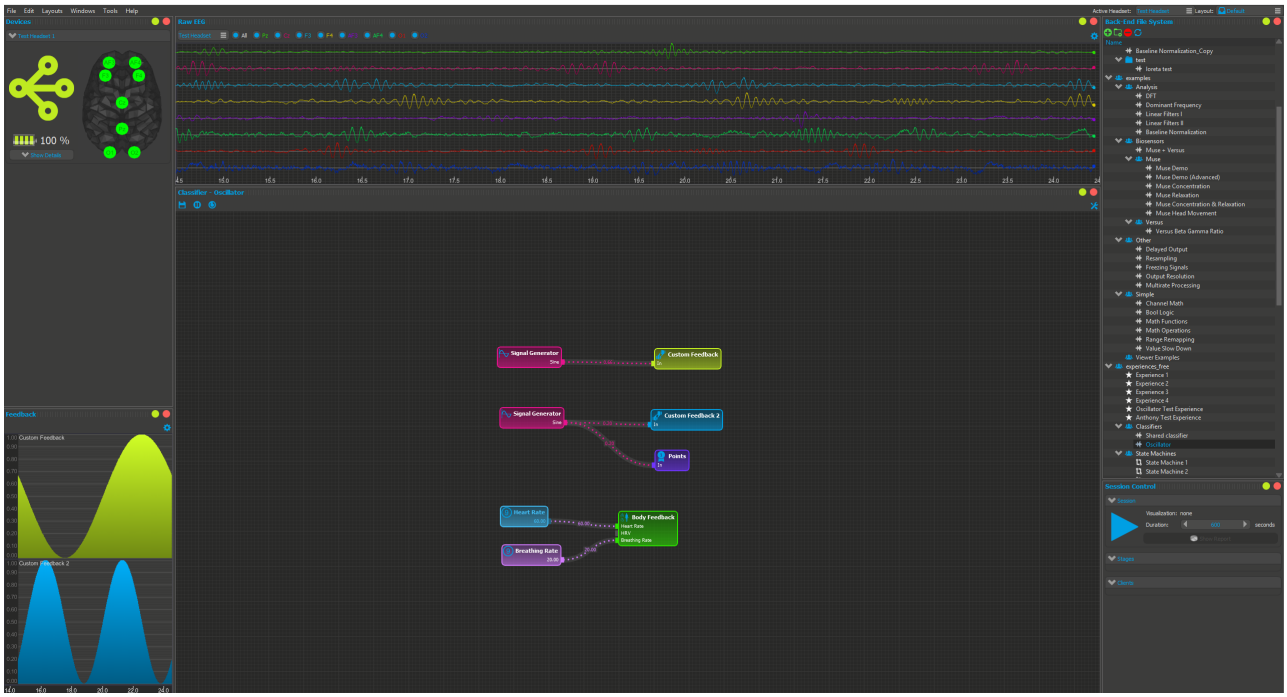

Figure 5.1: Screenshot of the neuromore Studio user interface. The top right window shows the connected BCI and its electrode placement. The bottom right window shows a feedback score measurement. The top middle window visualizes the received EEG data while the window in the bottom middle window shows the used classifier with its nodes. The top left window displays a file hierarchy while the bottom left window shows a session management window.

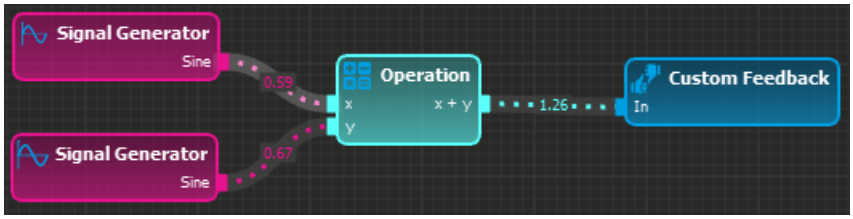

Figure 5.2: Simple classifier which uses an addition of sine functions as input to provide neurofeedback.

versions of the OpenBCI were integrated into neuromore Studio. An OpenBCI supporting up to sixteen electrodes is also used to evaluate the implemented algorithms. During the integration of the OpenBCI into neuromore Studio, an OpenBCI node is implemented which manages the Bluetooth connection between a PC and the OpenBCI. The OpenBCI node is able to retrieve the data from all electrodes at once or from selected electrodes only. Figure 5.3 shows an image of the OpenBCI and of the implemented OpenBCI node.

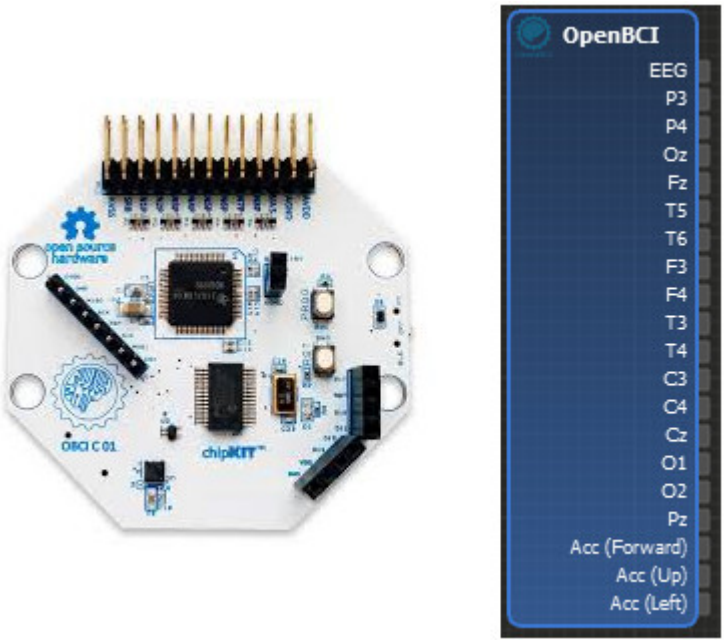

Figure 5.3: The right image shows the OpenBCI board while the left one shows the implemented OpenBCI node which can be used in neuromore Studio.

5.3 Electrode Placement Algorithm

For visualizing the electrical activity within a brain, electrodes are used to estimate the electrical current. An electrode value in correlation with the electrode position can then be used to map the calculated magnitudes of a pixel or voxel to a color. Electrode positions are usually denoted with an ID which helps recognizing the position of an electrode. Since electrodes are placed on a scalp, the easiest model to replicate a head is a sphere. Spherical coordinates can then be used to describe the electrode positions within a sphere. The spherical coordinates used in this project are retrieved from the New York State Psychiatric Institute[3], which provides more than 400 defined electrode positions.

5.3.1 Electrode Placement on a Two-Dimensional Surface

Spherical coordinates can be easily converted into two-dimensional Cartesian coordinates, which can then be placed on a surface. If two angles ϕ and θ as defined in Chapter 4 are known, the two-dimensional position vector can be calculated. This can be done by converting the

[3] psychophysiology.cpmc.columbia.edu/Software/CSDtoolbox/10-5-System_Mastoids_EGI129.csd

spherical coordinates into polar coordinates. The radius r can be estimated using the formula

$$r = \frac{|\phi|}{90} \tag{5.1}$$

The two-dimensional vector corresponding to the provided spherical coordinates can then be estimated using the formulas

$$x = r * \cos(\theta * \frac{\pi}{180}) \tag{5.2}$$

and

$$y = r * \sin(\theta * \frac{\pi}{180}) \tag{5.3}$$

A parser was created which converted the provided file into a comma separated file and also converted the spherical coordinates into two-dimensional coordinates using the formulas defined above. Since the comma separated file defines over 400 electrode positions, the parser was extended to create the source code for the used programming language in the project. Figure 5.4 shows images of the 10-20 and 10-10 electrode placement system, which are created using the provided coordinates and formulas in this section.

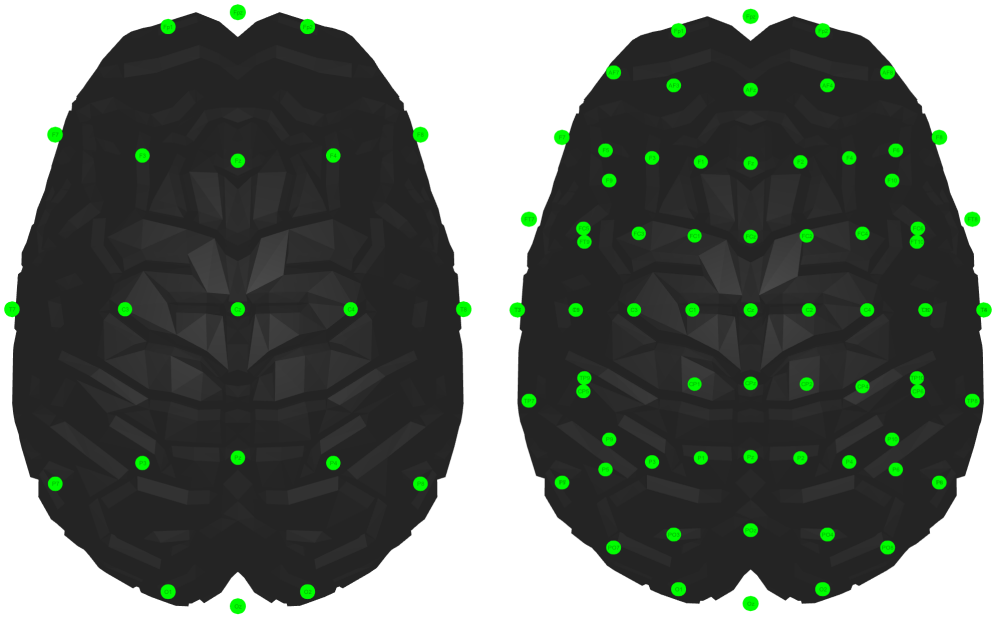

Figure 5.4: The implemented 10-20 and 10-10 electrode placement system on a two-dimensional surface. The left image shows the 10-20 electrode placement system while the right one shows the 10-10 electrode placement system.

5.3.2 Electrode Placement on a Three-Dimensional Sphere

The Cartesian coordinates of three-dimensional electrode positions can be calculated using the equations 4.3, 4.4 and 4.5. Figure 5.5 shows images of the 10-20 and 10-10 electrode placement system on a three-dimensional object.

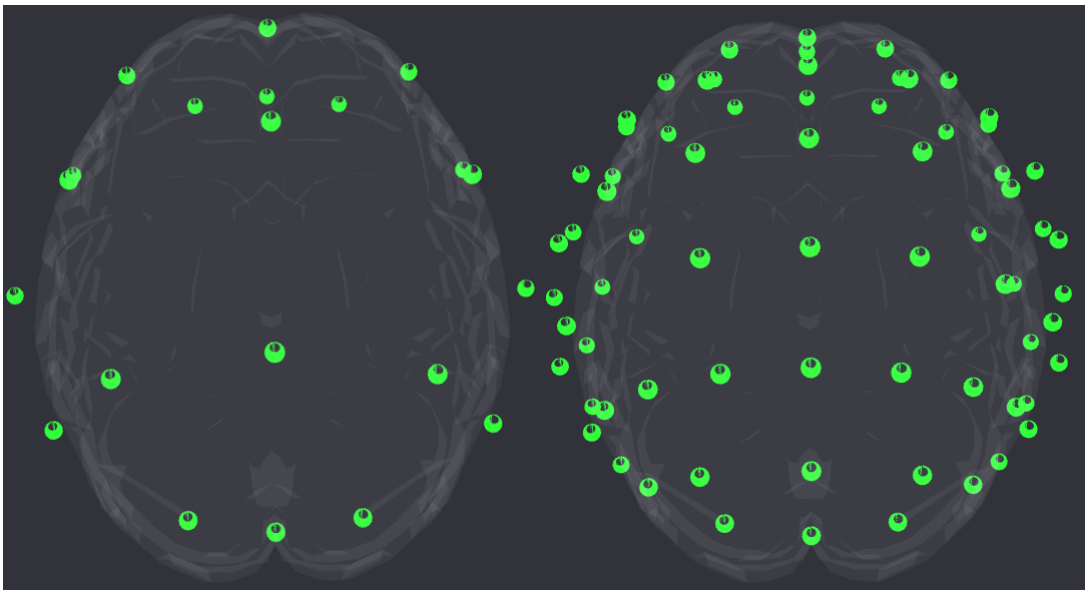

Figure 5.5: The implemented 10-20 and 10-10 electrode placement system on a three-dimensional object. The left image shows the 10-20 electrode placement system while the right one shows the 10-10 electrode placement system.

5.4 Two-Dimensional Heatmap

The algorithm stated with equation 4.6 is implemented to prove the correctness of its functionality regarding finding a solution to the forward problem. Because the algorithm follows a pixel-wise magnitude computation, the implementation slows down with increasing pixel density when computing it on the CPU in real-time. To overcome this drawback, the OpenGL Shading Language[4] (GLSL) is used to enable the processing of parallel workloads [LH07]. The result is a top view on a sphere from above, which uses a color coding to visualize the solution of the forward problem.

[4]www.opengl.org/wiki/OpenGL_Shading_Language

5.4.1 Verification

The heatmap is evaluated by simulating incoming current on defined electrodes. The current was normalized to a value in the range between $[0; 1]$ where 0 describes no electrical measurements while 1 denotes a high measured electrical activity. A spherical head model is used for the simulation. Figure 5.6 shows the visualized outcomes of this visualization.

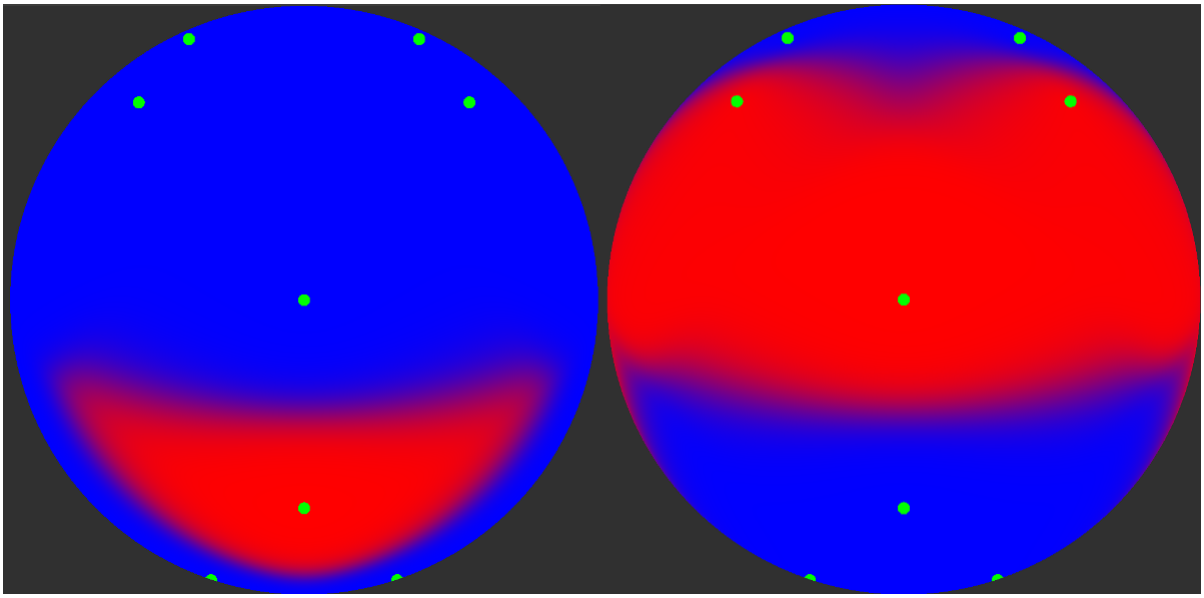

Figure 5.6: Heatmap which visualizes electrical measurements. The left heatmap shows strong electrical activity at one electrode with value 1, while the right heatmap visualizes strong electrical activity at three electrodes with value 1.

5.5 LORETA

As a solution to the inverse problem, a three-dimensional voxel-based real-time visualization has been developed using the sLORETA algorithm. This section covers already available software which implements sLORETA, a real-time implementation of it and a verification to prove its correctness.

5.5.1 sLORETA

This projects implements the sLORETA algorithm, which is known to have zero localization errors and being robust to noise. OpenGL[5] is used for performing vector-based hardware-accelerated drawing operations on the GPU. OpenCV[6] is used to perform matrix operations like matrix multiplication, matrix transposition or matrix inversion. The here presented implementation of sLORETA uses a spherical head model. The spherical head model is one of the easiest head models which allow reproducing experiments [Cuf96].

Each voxel consists of a cube having six quads and twelve triangles. These are arranged in a three-dimensional cubic lattice, where the granularity of the lattice is defined by an edge length provided by a user. The accuracy of the sLORETA calculations and the required computing power increase with a higher edge length. To overcome the problem of increasing computation time and freezing the UI thread, the sLORETA algorithm is computed on a separate thread. While the algorithm is processed, the UI thread prepares everything for the visualization. Each cell can also be colored with a magnitude to express the current power of a dipole moment. Figure 5.7 shows lattices for different edge lengths.

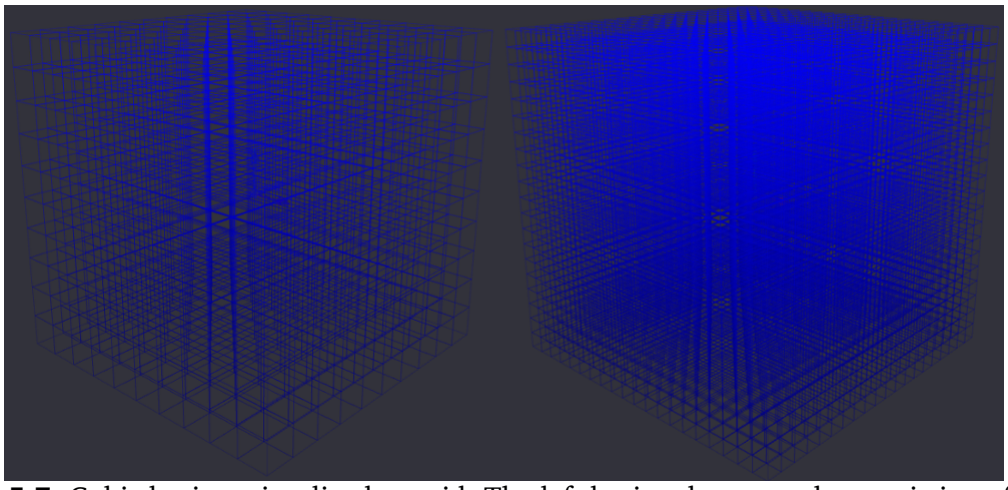

Figure 5.7: Cubic lattices visualized as grid. The left lattice shows a cube consisting of 10^3 cells while the right lattice consists of 20^3 cells.

Every dipole moment in the brain affects the density power of a voxel. The density of each voxel is represented by a three-dimensional vector. The length of the vector defines how strong a particular voxel is influenced by a dipole moment. The direction the vector describes the direction of the distribution of electrical current. Figure 5.8 shows a lattice with arrows, where a simulated dipole moment was placed in the middle of the lattice.

[5] www.opengl.org
[6] www.opencv.org

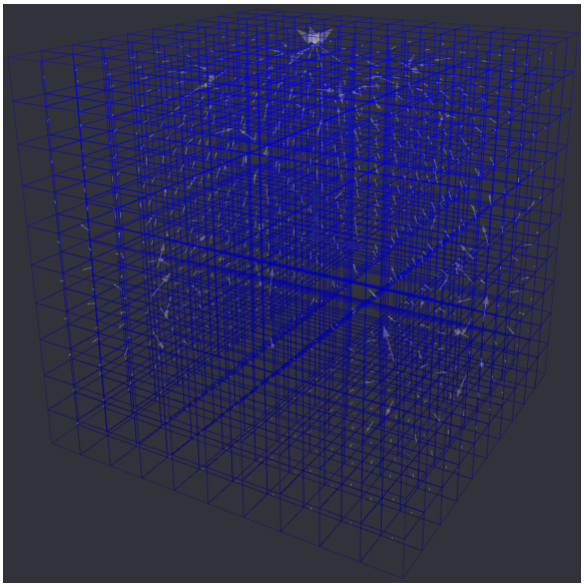

Figure 5.8: A lattice showing the distribution of electrical current with arrows. The direction of the arrows indicate the distribution of the electrical current.

The implementation of sLORETA also supports different parameters for modifying the representation of the visualization. The settings provide the functionality to set the edge length in voxels of the cubic lattice. A higher number also increases the accuracy of the rendering and requires therefore more computation power. The settings also provide the possibility to select a specific lobe which should be rendered. When a user is interested in a specific brain part, this part can be selected and can then be rendered with a high amount of voxels. Figure 5.9 shows the sLORETA rendering of a whole brain using 20^3 voxels and the sLORETA rendering of the frontal lobe using 30^3 voxels.

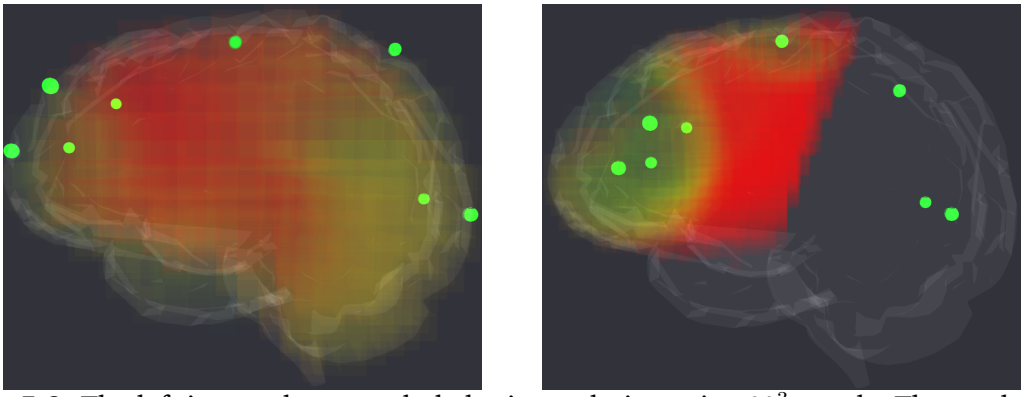

Figure 5.9: The left image shows a whole brain rendering using 20^3 voxels. The rendering requires high computation power and the voxels are coarse. The right image shows a frontal brain rendering using 30^3 voxels. The rendering requires high computation power, but the voxels are rendered finer.

The transparency of the outer voxels can be increased to enable a better view inside the brain. The regularization parameter and the conductivity are sLORETA specific parameter. The regularization parameter averages the magnitude of all voxels to being more robust against noise. The conductivity is a parameter with unit siemens per meter ($\frac{S}{m}$) which depends on the used electrodes and the conductivity of the scalp. The user can decide if the selected brain part and a human head can be rendered as useful guidance. At last, the color coding can be set. Figure 5.10 shows an image of all available settings.

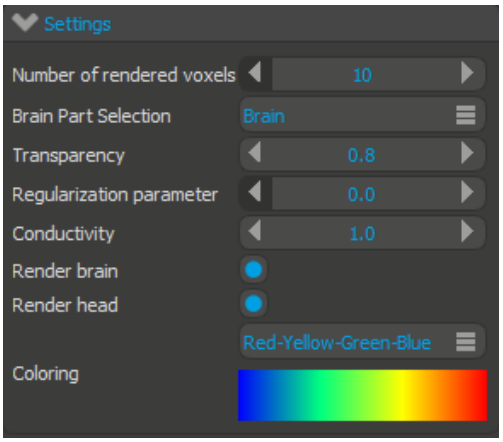

Figure 5.10: The supported sLORETA settings.

5.5.2 Verification

The verification of sLORETA is carried out using the Brain Electrical Source Analysis (BESA) Simulator[7] using thirty-three simulated electrodes. The BESA simulator is capable of defining arbitrary dipole moments within a brain. Defined dipole moment can be enriched with further information like the direction of electrical current or the frequency of their occurrence. These dipole moments can then be exported into a comma separated file which again can be read by neuromore Studio. A node was developed which enables to read in a comma separated file. sLORETA is used to recognize the dipole moments defined by the BESA simulator.

The verification is carried out in two steps. First, a single simulated dipole moment is placed inside the brain to validate a correct distribution of the current density power. Figure 5.11 shows an image of a simulated dipole moment in the middle of a brain directing inside the brain and its recognition using sLORETA.

The second verification step includes the recognition of two simulated dipole moments, each located in both brain hemispheres. The direction of the dipole moments point outside the brain

[7] www.besa.de/downloads/besa-simulator

and are placed in the middle of the brain. Figure 5.12 shows the simulated dipole moments in both brain hemispheres and their recognition using sLORETA.

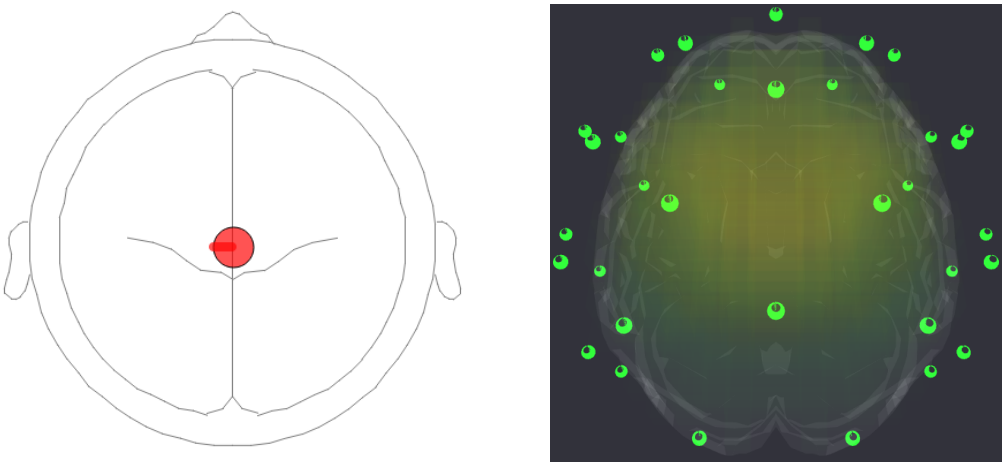

Figure 5.11: The left image shows a simulated dipole moment placed into the middle of a brain using the BESA simulator. The right image shows the corresponding sLORETA visualization.

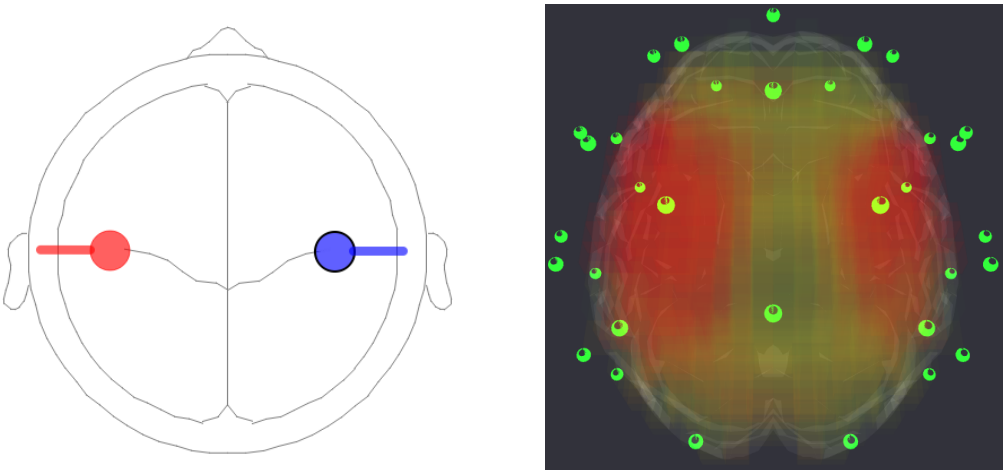

Figure 5.12: The left image shows two simulated dipole moments in each brain hemisphere using the BESA simulator. The right image shows the corresponding sLORETA visualization.

6 Evaluation

In this chapter, the implemented sLORETA algorithm will be evaluated. The results show, how sLORETA can be used to analyze the impact of a neurofeedback session on the brain. This chapter also presents a user study, which aims to increase brain activity in the frontal lobe using virtual reality and binaural sounds. The methodology, experimental setup, procedure of the study and the discussion of the results are covered as well.

6.1 Methodology

Related research has shown that the impact of drug addiction has negative effects on the brain regarding decreased brain activity and permanent brain damages. The excessive usage of drugs reduce brain activity, therefore may lead to depression and an aggressive behavior. Neurofeedback sessions aim to increase the activity in the brain.

Most neurofeedback sessions provide an input or a stimulus to a person to alter their brain activity. Feedback is generated to make the brain activity understandable to a person. For example, a visualization can be showed as input while alterations of the visualization could provide feedback to the person [PSV+03]. Other neurofeedback sessions use binaural sounds instead of visualizations to generate appropriate feedback [OJNZ13].

Binaural sounds produces a sine wave like audio with different frequencies on both ears. The brain detects the difference between both frequencies and produces a brain frequency which matches to the detected difference. It is shown that several brain lobes are connected with the auditory cortex and thus are influenced by binaural sounds [LKOM98, AWA+94]. In the context of drug addiction, people show decreased brain activity, especially in the frontal lobe [GV02]. With the usage of visualizations and binaural sounds a neurofeedback session can be created which trains the brain to increase brain activity.

The goal of the evaluation is to use the implemented sLORETA algorithm and its visualization to find differences in brain activation during a neurofeedback session. This includes a general increase of brain activity with focus at the frontal lobe for drug addiction treatment purposes.

A neurofeedback session with two input and output modalities is introduced to achieve these goals. A visualization and binaural sounds are used as input modalities, while alterations of the visualizations are performed depending on the EEG measurements. The visualization is

delivered using virtual reality to provide an immersive experience during the study. Binaural sounds are used to increase the brain activation in different brain parts.

The study itself consists of five tasks. EEG data is recorded for every task to enable a post hoc analysis.

For the first task, the participant is asked to keep their eyes open for three minutes to get an initial baseline of brain activity. Afterwards the eyes are closed for antoher three minutes to observe a possible boost of brain activation [BCJ+07, GBS+14].

The third task consists of a visualization using virtual reality in combination with binaural sounds as input variables to see if brain activation is altered. The visualization shows a tunnel which is traversed. The traversal speed increases with brain activation in the frontal lobe, while the color of the tunnel changes gradually from red to blue when brain activation in the occipital lobe is measured. The feedback is instantly made available to the user. The study also investigates the effects of virtual reality in the brain. The duration of the task lasts ten minutes.

Task four and five repeat the eyes-opened and eyes-closed, each for three minutes. This enables an analysis of impact from the neurofeedback session regarding the brain. Table 6.1 summarizes the procedure of the study.

Task	Duration in minutes	Task description	Environment
1	3	Eyes open	Dimmed room
2	3	Eyes closed	Dimmed room
3	10	Binaural sound and virtual reality	Virtual tunnel
4	3	Eyes open	Dimmed room
5	3	Eyes closed	Dimmed room

Table 6.1: Summarized procedure of the study.

6.2 Apparatus

The experimental setup consists of several devices and technologies which work together. The used brain sensing device is an OpenBCI board which supports up to sixteen electrodes at a sampling rate of 125 Hz. The OpenBCI is mounted on a 3D printed Ultracortex Mark 3[1] headset which eases the usage and compactness of the OpenBCI.

[1] www.github.com/OpenBCI/Ultracortex/tree/master/Mark_3

A suitable electrode placement was chosen to measure brain activity in motivation related parts of the brain such as the frontal lobe. The occipital lobe was taken into account as well to evaluate the impact of virtual reality on the visual processing parts of the brain.

Since the accuracy of the localization of electrical dipole moments increases with more electrodes, the other electrodes were equally distributed over the scalp. Figure 6.1 shows the Ultracortex together with the electrode placement which was used during the study.

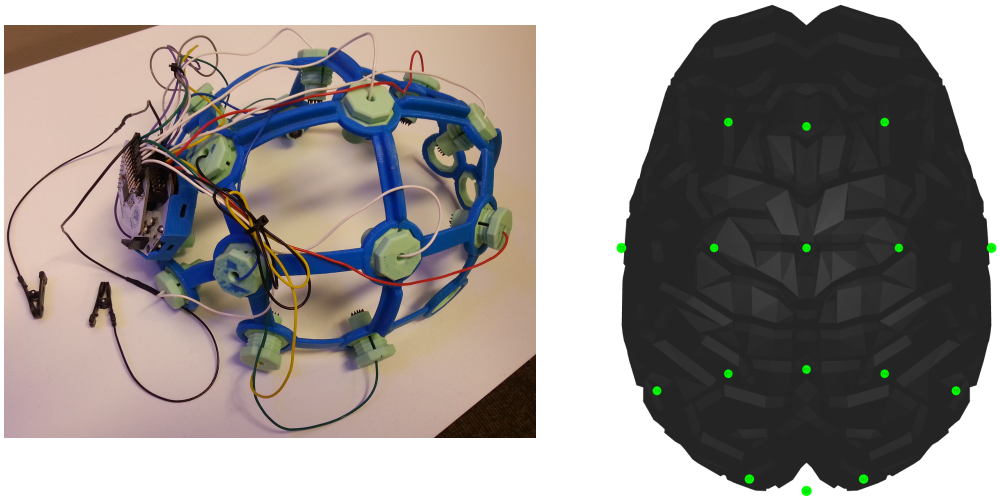

Figure 6.1: The left image shows the used Ultracortex Mark 3 while the right image shows the used electrode placement.

An Oculus Rift in combination with a visualization is used to provide immersive virtual reality feedback to the participant. The visualization is a tunnel which is traversed by a participant. The traversal speed increases when brain activation at the electrodes F3, F4 or Fz is measured. The color of the tunnel also changes gradually from red to blue with increasing brain activity at the electrodes O1, O2 and Oz. Figure 6.2 shows the red and blue tunnel used in the study.

The used binaural sound ranges from 175 Hz to 188 Hz in its frequency. The frequency of the binaural sound starts with 175 Hz at the left ear and with 182.5 Hz at the right ear, resulting in a difference of 7.5 Hz. Over a period of ten minutes, the frequency on the right ear increases to 188 Hz, hence producing waves between 7.5 Hz to 13 Hz.

The speed and color of the tunnel is influenced by the measured brain frequency. When brain activation in the frontal lobe is measured the speed of the tunnel increases, which enables the usage of a scoring system to reward the participant for being focused. When brain activation in the occipital lobe is measured, the tunnel changes its color gradually from red to blue. Figure 6.3 shows the used classifier responsible for the neurofeedback based on the measured brain data in neuromore Studio.

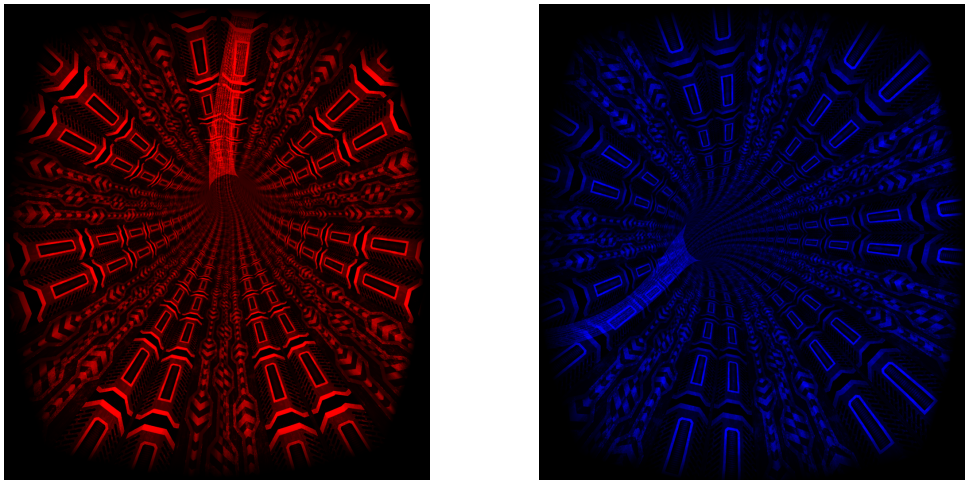

Figure 6.2: Tunnels used in the user study together with the Oculus Rift. The traversal speed of the tunnel depends on the brain activation at the frontal lobe. The color of the tunnel changes from red to blue with increasing brain activation at the occipital lobe. The left image shows a red tunnel, while the right image shows a blue tunnel.

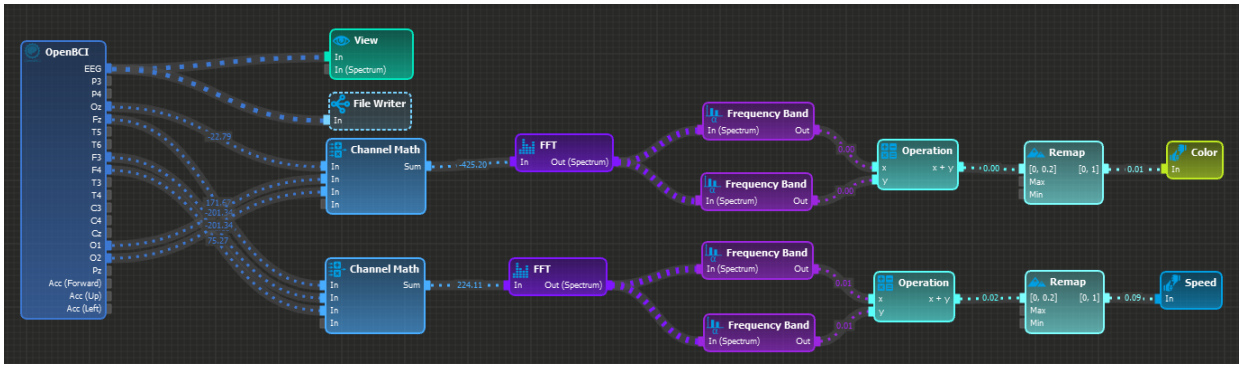

Figure 6.3: Classifier used in the study. The measured brain activation is summed up for the electrodes F3, F4 and Fz. A fast Fourier transform is applied to determine the alpha frequency using a frequency band which delivers values in the range $[0.0; 0.2]$. These are remapped to the range $[0.0; 1.0]$ and made available as speed factor, where 0.0 represents a slow tunnel traversal and 1.0 means a fast tunnel traversal. The same procedure is applied for the tunnel color using the electrodes O1, O2 and Oz.

6.3 Procedure

EEG measurements were recorded for every study session. Recorded sessions can then be replayed for post hoc analysis purposes. After the participant filled in the consent form and demographics. the participant was seated into a comfortable position. Additionally, the

participant was asked to move as less as possible for avoiding faulty measurements caused by muscle movements.

The study is divided into five tasks, where EEG data is recorded for every task using the OpenBCI together with the Ultracortex. The first and second task include the retrieval of a baseline of initial EEG brain data and resting conditions. The participant was asked to keep their eyes open for three minutes. For the second task, the participant was asked to close their eyes for three minutes to reach a calm state. Eye closure also causes a widespread power increase for a broad range of low frequencies [BCJ+07, GBS+14]. This improves the identification of impacts regarding brain activity of upcoming events. Furthermore, the differences in brain activation can be visualized afterwards. Both tasks were accomplished in a room with dimmed light.

The third task makes use of binaural sounds and an Oculus Rift to provide virtual reality based feedback depending on the measured EEG data. Additionally to the Ultracortex, the participant gets earphones playing the binaural sounds and an Oculus Rift mounted on their head. Figure 6.4 shows a participant wearing all mentioned devices during the study.

Figure 6.4: A participant using the Oculus Rift together with earphones and the Ultracortex.

The fourth and fifth task included the eyes-open and eyes-closed task again. The participant was asked to open its eyes for three minutes while recording EEG data. The fifth task repeats the eyes-closed task for another three minutes. The participants were interviewed afterwards. where they were asked how they feel and how they perceived the experience. Including the mounting time of all devices on the user, the duration of the study ranged between thirty and sixty minutes.

6.4 Results

Eight healthy male participants with an average age of 27.12 years resulting in a standard deviation of 5.19 years took part in the study. Their professions ranged from doctors and research assistants to data analysts and students. None of them participated in a bio- or neurofeedback study before. None of them were addicted to illicit drugs.

6.4.1 Qualitative Analysis

The analysis is carried out using the implemented sLORETA visualization to find differences regarding brain activity between every task. Twenty voxels are set as edge length for an increased level of detail. The conductivity is set to 0.025 $\frac{S}{m}$.

After the eyes-opened and eyes-closed task, all participants reported that they feel relaxed and comfortable. Visualization with sLORETA shows that the brain has an increased density power originating at the occipital lobe during the eyes-closed task. Figure 6.5 shows the sLORETA visualization during the eyes-opened and eyes-closed task. A red color indicates strong localized electrical activity proceeding with a transition over yellow and green to blue when the electrical power gets weaker. As stated by related research, the measured brain activity increases when the eyes are closed [GBS+14].

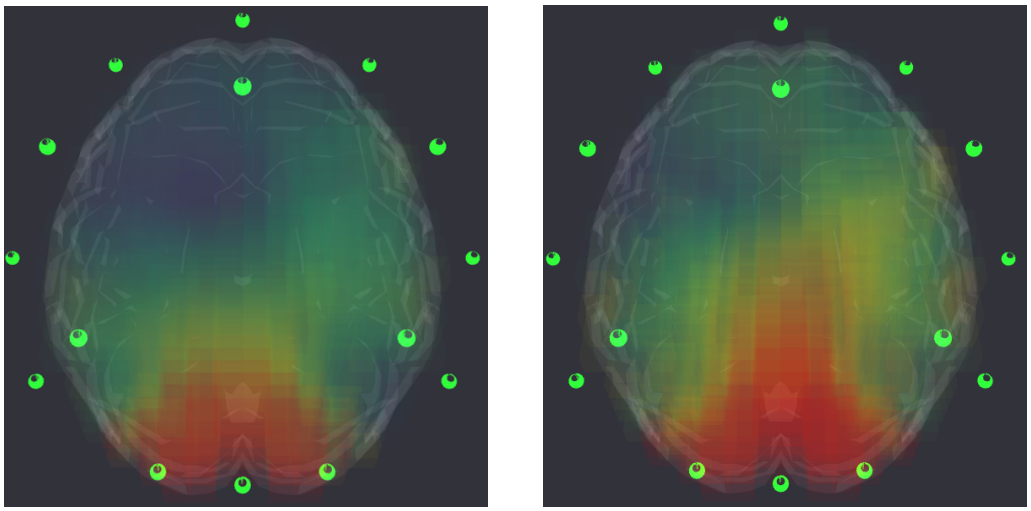

Figure 6.5: Localized dipole moments during the eyes-opened and eyes-closed task of participant one. The left image shows brain activation during the eyes-opened task while the right image shows brain activation during the eyes-closed task. Visual differences are visible between both tasks.

The virtual reality component using a tunnel including binaural sounds with alpha frequency also influenced the electrical dipole moments within a brain. Before the tunnel, the participant

stared in a blacked out Oculus Rift, thus seeing nothing. After the visualization, the participant stared in a blacked out Oculus Rift again. Increased activity in the frontal lobe, cerebellum and the occipital lobe can be noticed. Figure 6.6 shows a snapshot of the sLORETA visualization before and after the tunnel visualization.

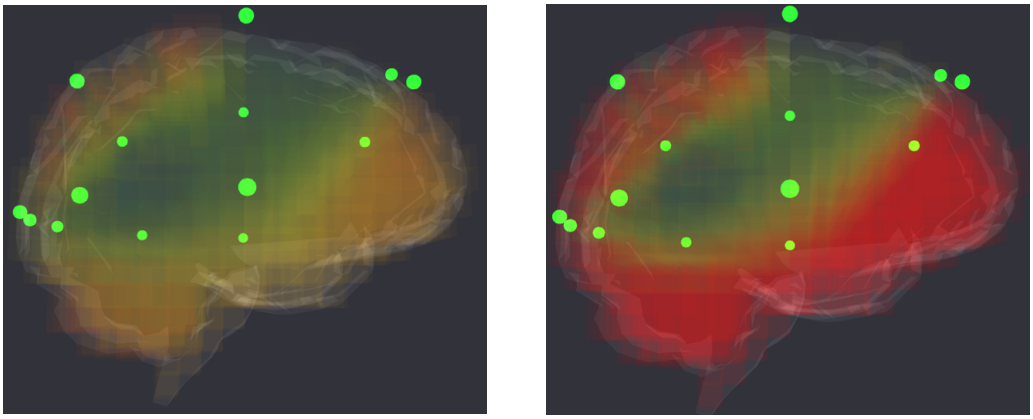

Figure 6.6: Differences in brain activation before and after the tunnel visualization of participant one. The left image shows brain activation before the tunnel visualization. The right image shows brain activation after the tunnel visualization.

After the tunnel visualization, the eyes-opened and eyes-closed task was repeated to find any visual differences. Figure 6.7 shows the visualized brain activation during the eyes-opened and eyes-closed task after the virtual reality task. More brain activation can be noticed than in the first eyes-opened and eyes-closed task. A difference is also visible before and after doing the virtual reality task during the eyes-opened and eyes-closed task. Overall, a slight increase of brain activity could be observed after people participated in the study.

Since all tasks were visually demanding , the sLORETA visualization showed permanent brain activation at the occipital lobe for all participants. No visual brain activity differences could be found between the different tasks.

The interview found out that most participants felt comfortable using the system. Especially after the eyes-opened and eyes-closed task the participants felt calm and relaxed. Using the Oculus Rift together with the Ultracortex is hard to achieve when tracking the complete frontal lobe since the frontal electrodes Fp1, Fp2 and Fpz interfere with the Oculus Rift. These electrodes were therefore left out for the study. The spiky electrodes of the Ultracortex began to hurt if they were placed too tight on the head. The binaural sound was accepted as comfortable.

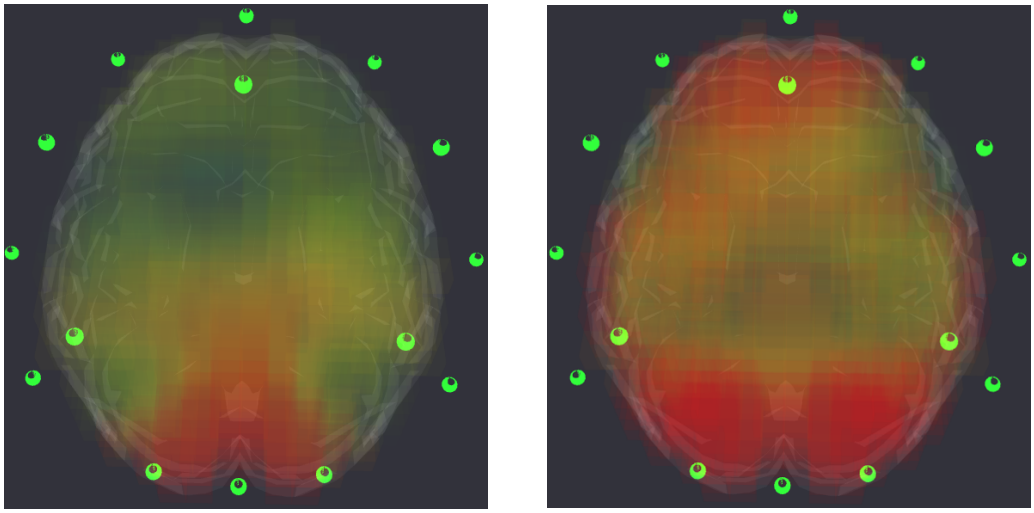

Figure 6.7: Brain activity after the virtual reality task during the eyes-opened and eyes-closed task of participant one. The left image shows brain activation during the eyes-opened task. The right image shows brain activation during the eyes-closed task. Visual differences are visible.

6.4.2 Quantitative Analysis

Since the study aims to increase the brain activity at the frontal lobe, the electrode F3, F4, Fz were chosen for quantitative analysis purposes. Since brain activation in the left hemisphere of the frontal lobe causes positive feelings, the focus lies on electrode F3 [TSRS81].

Figure 6.8 shows the line diagram containing the median of the measured microvolt values for every task of participant one. The median of the measured values in the first task at electrode F3 is 1.67 μV, while the measured median of electrode F3 at the last task is 60.01 μV, thus showing a great improvement. Figure 6.9 shows the result for another participant who was able to increase their brain activity. The median of the measured brain activity at electrode F3 improved from 10.93 μV to 30.15 μV except for some smaller values during the session.

A participant suffering from motion sickness has not showed an improvement at all, where the measured brain activity decreased over time. Overall, the values measured at electrode F3 fell from 34 μV to 6.26 μV. Figure 6.10 shows a corresponding line diagram of participant two.

Brain activation at the occipital lobe stayed constant for all participants since every task required visual activity. Switching colors during the tunnel visualization had no significant effect on brain activity.

A frequency analysis using a fast Fourier transform was not possible due to the high impedance of the spiky electrodes used together with the OpenBCI. An impedance check would have been necessary, which needs to be implemented before the study.

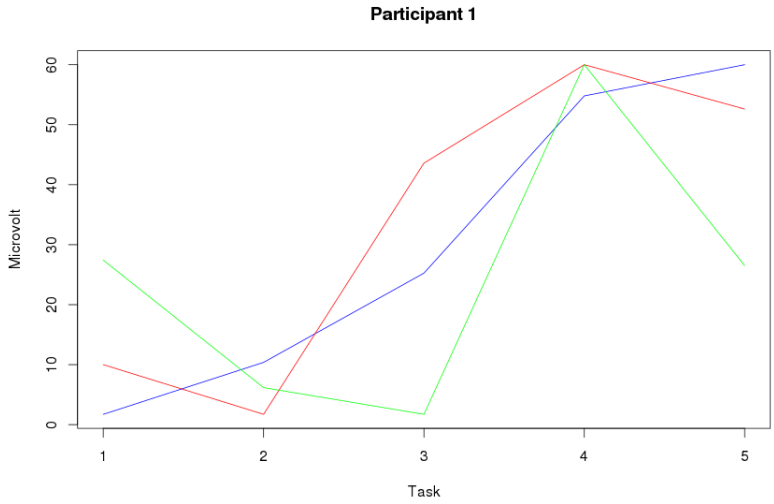

Figure 6.8: Measured brain activity at the electrode position F3, F4 and Fz of participant one. The blue line denotes electrode F3, the red line electrode F4 and the green line electrode Fz. The participant was able to increase their brain activity during the study.

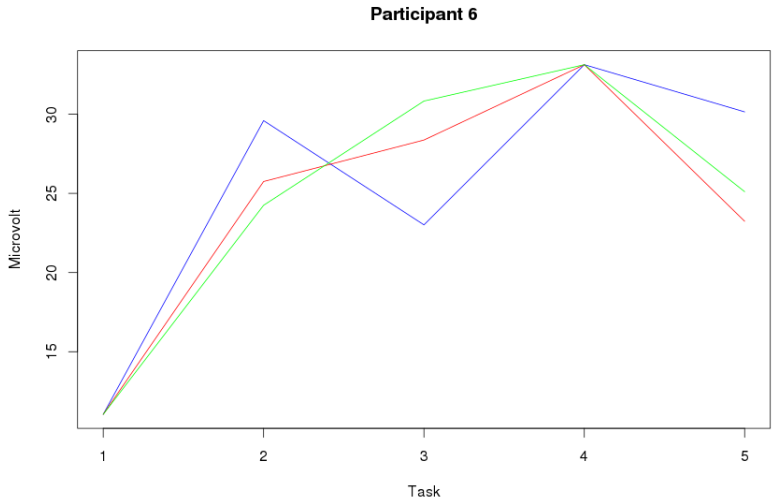

Figure 6.9: Measured brain activity at the electrode position F3, F4 and Fz of participant six. The blue line denotes electrode F3, the red line electrode F4 and the green line electrode Fz. The participant was able to increase their brain activity during the study.

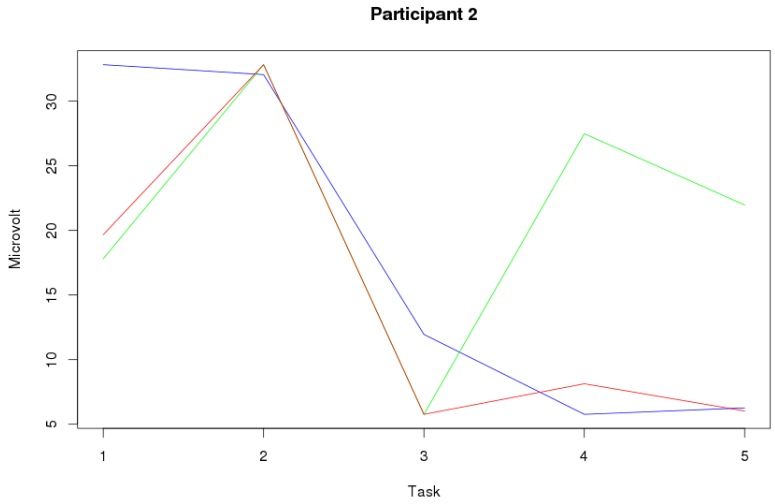

Figure 6.10: Measured brain activity at the electrode position F3, F4 and Fz of participant two. The blue line denotes electrode F3, the red line electrode F4 and the green line electrode Fz. The measured brain activity was not increased at all. The participant also suffered from motion sickness after the virtual reality task.

6.5 Discussion

Training the brain when participating in neurofeedback sessions is possible due to the latest technological advances. It strongly depends on the experience provided by the hardware and the neurofeedback session itself. To evaluate the usefulness of a neurofeedback session, often statistical methods are required.

The implemented sLORETA algorithm provides the possibility to get insight into brain activation and functionality without much effort. Eight participants participated in a developed neurofeedback session to evaluate the algorithm and the efficacy of the neurofeedback session itself. The neurofeedback session aims to increase brain activation, where substance abuse is associated with decreased brain activation in the frontal lobe.

Since all tasks were visual demanding, no brain activation differences regarding the occipital lobe could be found. Brain activation in the occipital lobe stayed constant.

In the first and second task, the participants were asked to remain calm while keeping their eyes opened or closed. While their eyes were opened, less brain activation could be measured than with closed eyes. This effect is already studied and proved in related research [BCJ+07, GBS+14]. All participants found it hard to remain calm, since they got bored while recording the EEG data without the virtual reality component.

Brain activation differences were found during the virtual reality task using binaural sounds. Almost all participants showed increased brain activity at the occipital and frontal lobe after the virtual reality session. Except of one participant, all participants felt comfortable and concentrated after the session. Furthermore, they could imagine to use the neurofeedback session as daily training. The binaural sound was not perceived as disturbance.

Participants who tried to force a speed up of the tunnel with concentration reported to be less successful than people which remained relaxed and only concentrated to the binaural sound. Forcing concentration under stress seems to make the result of the neurofeedback session worse.

A participant suffering from motion sickness showed significantly worse results. It is not clear what kind of impact the motion sickness has on the human brain.

The eyes-opened and eyes-closed task was performed directly afterwards to find any differences in brain activation caused by the virtual reality session. Seven participants showed higher brain activation in the eyes-opened and eyes-closed task than before doing the virtual reality task.

This observation is most probably a short-term effect, since the brain functionality does not change over a short period of time. Training the brain also requires a repetition of the proposed session, whereas at least ten sessions would be necessary to measure a significant long-term effect. Even then it is not sure if the training will last a lifetime.

6.6 Limitations

The results of the study can be influenced by certain factors. Fine grained structures in the brain can deliver different outcomes than the reported results. It is not easy to optimally set up the Ultracortex on every head form due to the lack of flexibility. Furthermore was a frequency analysis of the EEG data not possible due to the high impedance of the electrodes used with the OpenBCI.

The results can also be manipulated by small head movements, eye blinking or speaking. Natural noise also may spoil the result. To overcome these problems, averaging with the variance of the density power is accomplished as proposed by sLORETA. Of course, this procedure just minimizes the occurrence of noise in the result and is not completely eliminated.

Sometimes electrodes lost contact while sending data, thus resulting in loosing packages and data. The OpenBCI connected immediately again, but these short disconnects make it hard to retrieve exact and correct data. A high reliability is necessary, especially for medical applications.

While virtual reality simulates a world around a participant and tricks the brain in being in that world, the effects of binaural sound have not been proved. Several researcher reported

positive effects of binaural sound, but the studies suffer from many methodological weaknesses [LKOM98, RBH13, WCZ07].

7 Conclusion

The intention of this thesis was to create a three-dimensional visualization showing the distribution of electrical dipole moments within a human brain in real-time for neurofeedback purposes. The visualization was implemented using the sLORETA algorithm. The correctness was successfully proved with the usage of external tools. Furthermore, the algorithm was used to evaluate the usefulness of a proposed neurofeedback session for substance abuse treatment.

After a brief introduction, background knowledge was provided in Chapter 2 to prepare the reader for the following chapters. The functionality of the brain and selected topics from bioelectromagnetism were covered. Chapter 3 also gives a comprehensive overview of related work in this field of research.

Chapter 4 explains the mathematical and theoretical background of the presented visualizations. An algorithm for visualizing a solution to the forward problem was provided. The visualization itself can be presented as a two-dimensional heatmap with a top view on the head using a suitable color coding. Different LORETA algorithms were explained which solve the inverse problem. The sLORETA algorithm was chosen due to its simplicity, robustness to noise and real-time capabilities.

The technical realization and implementation of the original source localization algorithm was presented in Chapter 5. This chapter covers used hardware and software with neuromore Studio as base implementation. A verification was carried out to prove the correctness of the implemented algorithms. Different settings were made available to suit the visualization to the needs of a user.

An evaluation and the proposal for a neurofeedback session was presented in Chapter 6. The neurofeedback session aimed to increase brain activation , since substance abuse show a decreased distribution of brain activation. The study used an EEG tracking device, binaural sound and virtual reality using an Oculus Rift. The participants showed a higher occurrence of alpha waves in their brains after participating, although the effect will only last a short amount of time when not repeating the neurofeedback session. The analysis of the results was supported using the implemented sLORETA algorithm.

Analyzing EEG data can become complex with a high number of electrodes. Real-time analysis is almost impossible due to the amount of abstract data retrieved at once. Real-time visualizations help to close the gap between abstraction and concrete understanding.

The realized visualizations required an efficient implementation. Libraries which optimize the code using the GPU pipeline were used whenever possible. This efficient implementation makes it possible to evaluate the results coming from the EEG device in real-time.

The proposed neurofeedback session includes binaural sounds and virtual reality as supporting components. While the effects of virtual reality on the brain are currently being extensively researched, the effects of binaural sounds are still controversial. It is not known what kind of impact the binaural sounds have during neurofeedback sessions.

Wearing an Oculus Rift together with an EEG headset is difficult to accomplish but possible. Setting up the Ultracortex together with the Oculus Rift took some time, but most participants felt comfortable using the system during the study. Many participants were excited about the virtual reality component. While interviewing the participants, most of them stated a low degree of frustration. Many of them could speed up the tunnel after some minutes with higher alpha intensities.

The brain does not adapt to changes immediately. Neurofeedback sessions have to repeated over and over again to notice a long-term effect. Related research states at least ten repetitions to notice a long-term difference. It is not sure, for how long the training will last.

7.1 Future Work

Based on the work that has been done in this thesis, many improvements and extensions arise regarding the visualization and the proposed neurofeedback session.

The implementation of the visualizations are partly running on the CPU and the GPU. A complete shader-based implementation would help to compute the visualizations on the GPU, thus enabling a performance boost. The GPU is able to compute results with a couple of thousand computing units simultaneously.

The visualizations could also be tested with different EEG devices. Besides of simulations, the algorithms were only tested with the OpenBCI as real device.

The proposed neurofeedback session requires multiple sessions with the same participants carried out in regular intervals. The effects of the neurofeedback session need to be measured before and after the session for detecting differences.

The study also needs a control group, where participants are not using binaural sounds or are not told that the played sounds are actually binaural sounds. This could bring evidence about the usefulness of binaural sounds in neurofeedback sessions.

8 Acknowledgments

I take this opportunity to express my thankfulness to Prof. Dr. Albrecht Schmidt for giving me the possibility to work on such a great and interesting project which allowed me to get insight into other research fields. I also want to express my gratitude to Mariam Hassib and Dr. Deborah Mash for their valuable input and the knowledge I could get from our meetings. I thank the whole neuromore team, especially Benjamin Jillich, Manuel Jerger and Patrick Hilsbos, for their extensive support, their overwhelming collaboration, for the expertise I could obtain from their professional staff and the gained experience throughout this thesis.

Bibliography

[AHMG+15] Y. Abdelrahman, M. Hassib, M. Marquez Guinea, M. Funk, A. Schmidt. Implicit Engagement Detection for Interactive Museums Using Brain-Computer Interfaces. In *Extended Abstracts of the 17th International Conference on Human-computer Interaction with Mobile Devices and Services*, MobileHCI EA'15. ACM, New York, NY, USA, 2015. (Cited on page 10)

[ASF+07] E. Angelakis, S. Stathopoulou, J. L. Frymiare, D. L. Green, J. F. Lubar, J. Kounios. EEG neurofeedback: a brief overview and an example of peak alpha frequency training for cognitive enhancement in the elderly. *The Clinical Neuropsychologist*, 21(1):110–129, 2007. (Cited on pages 28 and 29)

[AWA+94] K. Alho, D. L. Woods, A. Algazi, R. Knight, R. Näätänen. Lesions of frontal cortex diminish the auditory mismatch negativity. *Electroencephalography and clinical neurophysiology*, 91(5):353–362, 1994. (Cited on page 55)

[BCJ+07] R. J. Barry, A. R. Clarke, S. J. Johnstone, C. A. Magee, J. A. Rushby. EEG differences between eyes-closed and eyes-open resting conditions. *Clinical Neurophysiology*, 118(12):2765–2773, 2007. (Cited on pages 56, 59 and 64)

[BCRW+99] S. Baron-Cohen, H. A. Ring, S. Wheelwright, E. T. Bullmore, M. J. Brammer, A. Simmons, S. C. Williams, et al. Social intelligence in the normal and autistic brain: an fMRI study. *European Journal of Neuroscience*, 11(6):1891–1898, 1999. (Cited on page 15)

[Boe] G. Boeree. General psychology - The neuron. *Annual review of psychology*. URL www.webspace.ship.edu/cgboer/theneuron.html. (Cited on pages 16 and 17)

[BSH98] D. Brown, A. W. Scheflin, D. C. Hammond. *Memory, trauma treatment, and the law*. WW Norton & Co, 1998. (Cited on page 29)

[CC91] R. N. Caine, G. Caine. Making connections: Teaching and the human brain. 1991. (Cited on page 15)

[Cen14] W. D. Center. LORETA Neurofeedback in Alcohol Use Disorders: A Case Study. *Z Score Neurofeedback: Clinical Applications*, 2014. (Cited on page 35)

[CJN+97] C. Chiron, I. Jambaque, R. Nabbout, R. Lounes, A. Syrota, O. Dulac. The right brain hemisphere is dominant in human infants. *Brain*, 120(6):1057–1065, 1997. (Cited on page 15)

[CLJ04] M. Congedo, J. F. Lubar, D. Joffe. Low-resolution electromagnetic tomography neurofeedback. *Neural Systems and Rehabilitation Engineering, IEEE Transactions on*, 12(4):387–397, 2004. (Cited on page 35)

[CLM10] R. Coben, M. Linden, T. E. Myers. Neurofeedback for autistic spectrum disorder: a review of the literature. *Applied psychophysiology and biofeedback*, 35(1):83–105, 2010. (Cited on page 9)

[CLSB08] R. Cannon, J. Lubar, E. Sokhadze, D. Baldwin. LORETA neurofeedback for addiction and the possible neurophysiology of psychological processes influenced: A case study and region of interest analysis of LORETA neurofeedback in right anterior cingulate cortex. *Journal of Neurotherapy*, 12(4):227–241, 2008. (Cited on page 34)

[CS95] C. B. Clayman, T. Smith. *The human body: An illustrated guide to its structure, function and disorders*. Stoddart, 1995. (Cited on page 15)

[Cuf96] B. N. Cuffin. EEG localization accuracy improvements using realistically shaped head models. *Biomedical Engineering, IEEE Transactions on*, 43(3):299–303, 1996. (Cited on page 51)

[DARN13] F. Dehghani-Arani, R. Rostami, H. Nadali. Neurofeedback training for opiate addiction: improvement of mental health and craving. *Applied psychophysiology and biofeedback*, 38(2):133–141, 2013. (Cited on page 32)

[Dav92] R. J. Davidson. Emotion and affective style: Hemispheric substrates. *Psychological science*, 3(1):39–43, 1992. (Cited on page 29)

[DB74] S. J. Dimond, J. Beaumont. *Hemisphere function in the human brain.* John Wiley & Sons, 1974. (Cited on page 15)

[DC13] R. Descartes, J. Cottingham. *René Descartes: Meditations on First Philosophy: With Selections from the Objections and Replies*. Cambridge University Press, 2013. (Cited on page 9)

[DH01] A. M. Dale, E. Halgren. Spatiotemporal mapping of brain activity by integration of multiple imaging modalities. *Current opinion in neurobiology*, 11(2):202–208, 2001. (Cited on page 20)

[DLF+00] A. M. Dale, A. K. Liu, B. R. Fischl, R. L. Buckner, J. W. Belliveau, J. D. Lewine, E. Halgren. Dynamic statistical parametric mapping: combining fMRI and MEG for high-resolution imaging of cortical activity. *Neuron*, 26(1):55–67, 2000. (Cited on page 33)

[Ecc13] J. C. Eccles. *The cerebellum as a neuronal machine*. Springer Science & Business Media, 2013. (Cited on page 15)

[FLRT01] T. C. Ferree, P. Luu, G. S. Russell, D. M. Tucker. Scalp electrode impedance, infection risk, and EEG data quality. *Clinical Neurophysiology*, 112(3):536–544, 2001. (Cited on page 16)

[Fou] W. Foundation. Wikimedia Foundation. *Wikimedia Foundation*. URL upload.wikimedia.org/wikipedia/commons/d/dc/3D_Spherical_2.svg. (Cited on page 38)

[FR13] M. Funk, M. Raschke. Brain Painting: Action Paintings based on BCI-Input. In *Mensch & Computer 2013*, volume 2013. 2013. (Cited on page 10)

[Gar76] I. Gartha. What is biofeedback? *Canadian Family Physician*, 22:105, 1976. (Cited on page 13)

[GBS+14] A. S. Geller, J. F. Burke, M. R. Sperling, A. D. Sharan, B. Litt, G. H. Baltuch, T. H. Lucas, M. J. Kahana. Eye closure causes widespread low-frequency power increase and focal gamma attenuation in the human electrocorticogram. *Clinical Neurophysiology*, 125(9):1764–1773, 2014. (Cited on pages 56, 59, 60 and 64)

[GC99] D. J. Griffiths, R. College. *Introduction to electrodynamics*, volume 3. prentice Hall Upper Saddle River, NJ, 1999. (Cited on page 20)

[GIS+10] J. Gruzelier, A. Inoue, R. Smart, A. Steed, T. Steffert. Acting performance and flow state enhanced with sensory-motor rhythm neurofeedback comparing ecologically valid immersive VR and training screen scenarios. *Neuroscience Letters*, 480(2):112–116, 2010. (Cited on page 30)

[Gol12] J. S. Golan. Moore–Penrose Pseudoinverses. In *The Linear Algebra a Beginning Graduate Student Ought to Know*, pp. 441–452. Springer, 2012. (Cited on page 41)

[GV02] R. Z. Goldstein, N. D. Volkow. Drug addiction and its underlying neurobiological basis: neuroimaging evidence for the involvement of the frontal cortex. *American Journal of Psychiatry*, 159(10):1642–1652, 2002. (Cited on pages 25 and 55)

[Ham00] D. C. Hammond. Neurofeedback treatment of depression with the Roshi. *Journal of Neurotherapy*, 4(2):45–56, 2000. (Cited on page 29)

[Ham03] D. C. Hammond. QEEG-guided neurofeedback in the treatment of obsessive compulsive disorder. *Journal of Neurotherapy*, 7(2):25–52, 2003. (Cited on page 29)

[Ham05] D. C. Hammond. Neurofeedback treatment of depression and anxiety. *Journal of Adult Development*, 12(2-3):131–137, 2005. (Cited on page 29)

[Ham07] D. C. Hammond. What is neurofeedback? *Journal of Neurotherapy*, 10(4):25–36, 2007. (Cited on pages 14 and 27)

[HEBB+10] T. Horrell, A. El-Baz, J. Baruth, A. Tasman, G. Sokhadze, C. Stewart, E. Sokhadze. Neurofeedback effects on evoked and induced EEG gamma band reactivity to drug-related cues in cocaine addiction. *Journal of neurotherapy*, 14(3):195–216, 2010. (Cited on pages 30 and 31)

[HEM95] W. Heller, M. A. Etienne, G. A. Miller. Patterns of perceptual asymmetry in depression and anxiety: implications for neuropsychological models of emotion and psychopathology. *Journal of abnormal psychology*, 104(2):327, 1995. (Cited on page 29)

[HGS07] H. Heinrich, H. Gevensleben, U. Strehl. Annotation: Neurofeedback–train your brain to train behaviour. *Journal of Child Psychology and Psychiatry*, 48(1):3–16, 2007. (Cited on pages 30 and 31)

[HHI+93] M. Hämäläinen, R. Hari, R. J. Ilmoniemi, J. Knuutila, O. V. Lounasmaa. Magnetoencephalography—theory, instrumentation, and applications to noninvasive studies of the working human brain. *Reviews of modern Physics*, 65(2):413, 1993. (Cited on page 20)

[HI84] M. S. Hämäläinen, R. J. Ilmoniemi. *Interpreting measured magnetic fields of the brain: estimates of current distributions*. Helsinki University of Technology, Department of Technical Physics, 1984. (Cited on page 32)

[HM01] S. E. Hyman, R. C. Malenka. Addiction and the brain: the neurobiology of compulsion and its persistence. *Nature reviews neuroscience*, 2(10):695–703, 2001. (Cited on page 10)

[HS03] P. N. Hoaken, S. H. Stewart. Drugs of abuse and the elicitation of human aggressive behavior. *Addictive behaviors*, 28(9):1533–1554, 2003. (Cited on page 24)

[HVG+07] H. Hallez, B. Vanrumste, R. Grech, J. Muscat, W. De Clercq, A. Vergult, Y. D'Asseler, K. P. Camilleri, S. G. Fabri, S. Van Huffel, et al. Review on solving the forward problem in EEG source analysis. *Journal of neuroengineering and rehabilitation*, 4(1):46, 2007. (Cited on page 24)

[Ilm93] R. Ilmoniemi. Models of source currents in the brain. *Brain topography*, 5(4):331–336, 1993. (Cited on page 40)

[JKMF14] M. A. Jatoi, N. Kamel, A. S. Malik, I. Faye. EEG based brain source localization comparison of sLORETA and eLORETA. *Australasian Physical & Engineering Sciences in Medicine*, 37(4):713–721, 2014. (Cited on page 34)

[JTD07] V. Jurcak, D. Tsuzuki, I. Dan. 10/20, 10/10, and 10/5 systems revisited: their validity as relative head-surface-based positioning systems. *Neuroimage*, 34(4):1600–1611, 2007. (Cited on page 21)

[KBKE99] W. E. Kincses, C. Braun, S. Kaiser, T. Elbert. Modeling extended sources of event-related potentials using anatomical and physiological constraints. 1999. (Cited on page 32)

[Kim00] J. Kim. *Mind in a physical world: An essay on the mind-body problem and mental causation*. MIT press, 2000. (Cited on page 9)

[LBZ+00] H. Lodish, A. Berk, S. L. Zipursky, P. Matsudaira, D. Baltimore, J. Darnell, et al. Overview of neuron structure and function. 2000. (Cited on page 16)

[Les97] A. I. Leshner. Addiction is a brain disease, and it matters. *Science*, 278(5335):45–47, 1997. (Cited on page 24)

[LH07] D. Luebke, G. Humphreys. How gpus work. *Computer*, (2):96–100, 2007. (Cited on page 49)

[LHJ+12] D. Linden, I. Habes, S. J. Johnston, S. Linden, R. Tatineni, L. Subramanian, B. Sorger, D. Healy, R. Goebel. Real-time self-regulation of emotion networks in patients with depression. *PloS one*, 7(6):e38115, 2012. (Cited on page 9)

[LKOM98] J. D. Lane, S. J. Kasian, J. E. Owens, G. R. Marsh. Binaural auditory beats affect vigilance performance and mood. *Physiology & behavior*, 63(2):249–252, 1998. (Cited on pages 55 and 66)

[LLPG98] J. Le, M. Lu, E. Pellouchoud, A. Gevins. A rapid method for determining standard 10/10 electrode positions for high resolution EEG studies. *Electroencephalography and clinical Neurophysiology*, 106(6):554–558, 1998. (Cited on page 21)

[LSN+81] J. F. Lubar, H. S. Shabsin, S. E. Natelson, G. S. Holder, S. F. Whitsett, W. E. Pamplin, D. I. Krulikowski. EEG operant conditioning in intractable epileptics. *Archives of Neurology*, 38(11):700–704, 1981. (Cited on page 30)

[Lyv00] M. Lyvers. " Loss of control" in alcoholism and drug addiction: a neuroscientific interpretation. *Experimental and clinical psychopharmacology*, 8(2):225, 2000. (Cited on page 10)

[Mil78] N. E. Miller. Biofeedback and visceral learning. *Annual review of psychology*, 29(1):373–404, 1978. (Cited on page 13)

[MLL99] J. C. Mosher, R. M. Leahy, P. S. Lewis. EEG and MEG: forward solutions for inverse methods. *Biomedical Engineering, IEEE Transactions on*, 46(3):245–259, 1999. (Cited on page 24)

[MP95] J. Malmivuo, R. Plonsey. *Bioelectromagnetism: principles and applications of bioelectric and biomagnetic fields*. Oxford university press, 1995. (Cited on pages 22 and 23)

[MPL+99] C. M. Michel, R. G. de Peralta, G. Lantz, S. G. Andino, L. Spinelli, O. Blanke, T. Landis, M. Seeck. Spatiotemporal EEG analysis and distributed source estimation in presurgical epilepsy evaluation. *Journal of clinical neurophysiology*, 16(3):239–266, 1999. (Cited on page 32)

[MS98] F. A. Middleton, P. L. Strick. The cerebellum: an overview. *Trends in cognitive sciences*, 2(9):305–306, 1998. (Cited on page 15)

[NM07] Y. Nestoriuc, A. Martin. Efficacy of biofeedback for migraine: a meta-analysis. *Pain*, 128(1):111–127, 2007. (Cited on page 9)

[NS05] E. Niedermeyer, F. L. da Silva. *Electroencephalography: basic principles, clinical applications, and related fields*. Lippincott Williams & Wilkins, 2005. (Cited on page 21)

[NS06] P. L. Nunez, R. Srinivasan. *Electric fields of the brain: the neurophysics of EEG*. Oxford university press, 2006. (Cited on page 21)

[OJNZ13] F. On, R. Jailani, H. Norhazman, N. M. Zaini. Binaural beat effect on brainwaves based on EEG. In *Signal Processing and its Applications (CSPA), 2013 IEEE 9th International Colloquium on*, pp. 339–343. IEEE, 2013. (Cited on page 55)

[Oub02] A. Oubré. EEG neurofeedback for treating psychiatric disorders. *Psychiatric Times*, 19(2), 2002. (Cited on page 27)

[PM99] R. D. Pascual-Marqui. Review of methods for solving the EEG inverse problem. *International journal of bioelectromagnetism*, 1(1):75–86, 1999. (Cited on page 32)

[PM+02] R. D. Pascual-Marqui, et al. Standardized low-resolution brain electromagnetic tomography (sLORETA): technical details. *Methods Find Exp Clin Pharmacol*, 24(Suppl D):5–12, 2002. (Cited on pages 23, 33 and 42)

[PM07] R. D. Pascual-Marqui. Discrete, 3D distributed, linear imaging methods of electric neuronal activity. Part 1: exact, zero error localization. *arXiv preprint arXiv:0710.3341*, 2007. (Cited on pages 33 and 43)

[PMA00] R. G. de Peralta Menendez, S. L. G. Andino. Discussing the capabilities of Laplacian minimization. *Brain topography*, 13(2):97–104, 2000. (Cited on page 32)

[PMEK+02] R. D. Pascual-Marqui, M. Esslen, K. Kochi, D. Lehmann, et al. Functional imaging with low-resolution brain electromagnetic tomography (LORETA): a review. *Methods and findings in experimental and clinical pharmacology*, 24(Suppl C):91–95, 2002. (Cited on page 33)

[PMLK+99] R. D. Pascual-Marqui, D. Lehmann, T. Koenig, K. Kochi, M. C. Merlo, D. Hell, M. Koukkou. Low resolution brain electromagnetic tomography (LORETA) functional imaging in acute, neuroleptic-naive, first-episode, productive schizophrenia. *Psychiatry Research: Neuroimaging*, 90(3):169–179, 1999. (Cited on page 33)

[PMML94] R. D. Pascual-Marqui, C. M. Michel, D. Lehmann. Low resolution electromagnetic tomography: a new method for localizing electrical activity in the brain. *International Journal of psychophysiology*, 18(1):49–65, 1994. (Cited on pages 32, 40 and 42)

[PSV+03] J. Pineda, D. S. Silverman, A. Vankov, J. Hestenes, et al. Learning to control brain rhythms: making a brain-computer interface possible. *Neural Systems and Rehabilitation Engineering, IEEE Transactions on*, 11(2):181–184, 2003. (Cited on page 55)

[Puc06] H. L. Puckhaber. *New Research on Biofeedback*. Nova Publishers, 2006. (Cited on page 14)

[PZ14] F. Peng, L. Zhang. Prolonged menstruation and increased menstrual blood with generalized δ electroencephalogram power: A case report. *Experimental and therapeutic medicine*, 7(3):728–730, 2014. (Cited on page 21)

[RBH13] S. A. Reedijk, A. Bolders, B. Hommel. The impact of binaural beats on creativity. *Frontiers in human neuroscience*, 7, 2013. (Cited on page 66)

[RE99] T. W. Robbins, B. J. Everitt. Drug addiction: bad habits add up. *Nature*, 398(6728):567–570, 1999. (Cited on page 25)

[REE08] T. Robbins, K. Ersche, B. Everitt. Drug addiction and the memory systems of the brain. *Annals of the New York Academy of Sciences*, 1141(1):1–21, 2008. (Cited on page 24)

[SHJ+11] L. Subramanian, J. V. Hindle, S. Johnston, M. V. Roberts, M. Husain, R. Goebel, D. Linden. Real-time functional magnetic resonance imaging neurofeedback for treatment of Parkinson's disease. *The Journal of Neuroscience*, 31(45):16309–16317, 2011. (Cited on pages 27 and 28)

[SJ13] R. Serway, J. Jewett. *Physics for scientists and engineers with modern physics*. Cengage learning, 2013. (Cited on pages 18 and 19)

[SP95] E. Saxby, E. G. Peniston. Alpha-theta brainwave neurofeedback training: An effective treatment for male and female alcoholics with depressive symptoms. *Journal of clinical psychology*, 51(5):685–693, 1995. (Cited on page 30)

[SSFP+12] A. Sahami Shirazi, M. Funk, F. Pfleiderer, H. Glück, A. Schmidt. *MediaBrain: Annotating Videos based on Brain-Computer Interaction*, pp. 263–272. Oldenbourg Wissenschaftsverlag, 2012. doi:doi:10.1524/9783486718782.263. (Cited on page 10)

[SSH07] T. M. Sokhadze, C. M. Stewart, M. Hollifield. Integrating cognitive neuroscience research and cognitive behavioral treatment with neurofeedback therapy in drug addiction comorbid with Posttraumatic Stress Disorder: A conceptual review. *Journal of Neurotherapy*, 11(2):13–44, 2007. (Cited on page 27)

[ST82] M. D. Stanton, T. C. Todd. *The family therapy of drug abuse and addiction*. Guilford Press, 1982. (Cited on page 25)

[Ste00] M. B. Sterman. Basic concepts and clinical findings in the treatment of seizure disorders with EEG operant conditioning. *Clinical EEG and Neuroscience*, 31(1):45–55, 2000. (Cited on page 30)

[Ste02] D. J. Stein. Obsessive-compulsive disorder. *The Lancet*, 360(9330):397–405, 2002. (Cited on page 28)

[Tep02] M. Teplan. Fundamentals of EEG measurement. *Measurement science review*, 2(2):1–11, 2002. (Cited on pages 17 and 18)

[TSBP95] I. Tarkka, D. Stokić, L. Basile, A. Papanicolaou. Electric source localization of the auditory P300 agrees with magnetic source localization. *Electroencephalography and Clinical Neurophysiology/Evoked Potentials Section*, 96(6):538–545, 1995. (Cited on page 32)

[TSRS81] M. Tucker, C. E. Stenslie, R. S. Roth, S. L. Shearer. Right frontal lobe activation and right hemisphere performance: Decrement during a depressed mood. *Archives of General Psychiatry*, 38(2):169–174, 1981. (Cited on page 62)

[TTH+09] G. Tan, J. Thornby, D. C. Hammond, U. Strehl, B. Canady, K. Arnemann, D. A. Kaiser. Meta-analysis of EEG biofeedback in treating epilepsy. *Clinical EEG and Neuroscience*, 40(3):173–179, 2009. (Cited on page 9)

[WCZ07] H. Wahbeh, C. Calabrese, H. Zwickey. Binaural beat technology in humans: a pilot study to assess psychologic and physiologic effects. *The Journal of Alternative and Complementary Medicine*, 13(1):25–32, 2007. (Cited on page 66)

[WGW93] J. P. Wikswo, A. Gevins, S. J. Williamson. The future of the EEG and MEG. *Electroencephalography and clinical Neurophysiology*, 87(1):1–9, 1993. (Cited on page 40)

[WK05] J. E. Walker, G. P. Kozlowski. Neurofeedback treatment of epilepsy. *Child and adolescent psychiatric clinics of North America*, 14(1):163–176, 2005. (Cited on page 30)

[WLKK91] S. J. Williamson, Z.-L. Lü, D. Karron, L. Kaufman. Advantages and limitations of magnetic source imaging. *Brain topography*, 4(2):169–180, 1991. (Cited on page 20)

All links were last followed on November 30, 2015.

Declaration

I hereby declare that the work presented in this thesis is entirely my own and that I did not use any other sources and references than the listed ones. I have marked all direct or indirect statements from other sources contained therein as quotations. Neither this work nor significant parts of it were part of another examination procedure. I have not published this work in whole or in part before. The electronic copy is consistent with all submitted copies.

---

place, date, signature